

RESOURCE AWARE ADAPTIVE BINARY QUANTIZER DESIGN FOR TARGET
TRACKING IN WIRELESS SENSOR NETWORKS



by
Abdulkadir Köse

Submitted to Graduate School of Natural and Applied Sciences
in Partial Fulfillment of the Requirements
for the Degree of Master of Science in
Electrical and Electronics Engineering

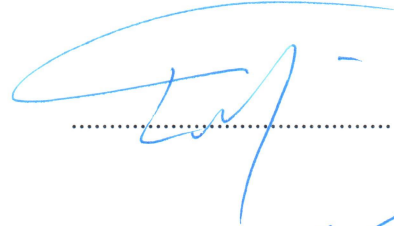
Yeditepe University

2016

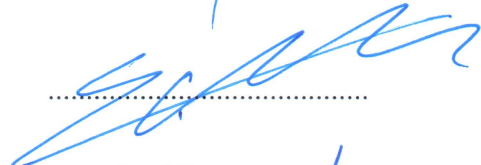
RESOURCE AWARE ADAPTIVE BINARY QUANTIZER DESIGN FOR TARGET
TRACKING IN WIRELESS SENSOR NETWORKS

APPROVED BY:

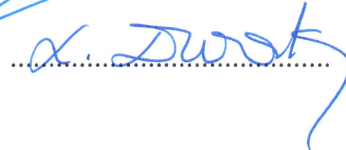
Assist. Prof. Dr. Engin Maşazade
(Thesis Supervisor)



Prof. Dr. Cem Ünsalan



Assoc. Prof. Dr. Lütfiye Durak Ata



DATE OF APPROVAL: /.... /2016

ACKNOWLEDGEMENTS

First and foremost, I would like to express my sincere gratitude to my advisor Engin Maşazade for the continuous support of my project, for his patience, motivation, enthusiasm, and immense knowledge. His guidance helped me in all the time of research and writing of this thesis.

I would like to thank Prof. Cem Ünsalan for being a committee member and his support throughout my study at Yeditepe University. I would like to thank Assoc. Prof. Lütfiye Durak Ata also for being a committee member.

In addition, my special thanks to my friends Volkan Talha Doğukan and Veysel Yaman Akgün.

I thank to my lovely parents for their endless patience and encouragements at all conditions in my life.

Finally, I am grateful to The Scientific and Technological Research Council of Turkey (TUBITAK) which support this project under Grant 113E220.

ABSTRACT

RESOURCE AWARE ADAPTIVE BINARY QUANTIZER DESIGN FOR TARGET TRACKING IN WIRELESS SENSOR NETWORKS

In this thesis, we design a resource aware adaptive binary quantizer for tracking a moving target in a Wireless Sensor Network (WSN). Due to stringent WSN resources, such as node energy or communication bandwidth, rather than transmitting the analog sensor measurements, sensors first preprocess their measurements and then send binary quantized versions of their measurements either directly (Single-hop transmission) or via cluster heads (2-hop transmission) to the Fusion Center (FC). Firstly, at each time step of tracking, the local decision thresholds of sensors are obtained optimally and dynamically as a result of a Multiobjective Optimization Problem (MOP). The considered MOP jointly minimizes the estimation error and number of sensor transmitting to FC under Single-hop links. Secondly, while considering energy depletion in hardware of sensors during transmission, we also formulate MOP to minimize the total energy consumption of the WSN under Single-hop and 2-hop links. As well as MOP, we also prefer Minimum Transmission Energy Path (MTEP) based transmission where sensors' observations follow less energy required path which can be either Single-hop or 2-hop path to reach the FC. Numerical results show that significant savings in both total energy consumption of WSN and the average number of sensors transmitting to the FC are provided while keeping good target tracking performance. Finally, we propose a proportional Time Division Multiple Access (TDMA) based medium access control (MAC) approach where the time allocated to each sensor to transmit its binary decision to the FC becomes related with the value of its measurement while considering wireless channel impairments under Single-hop links. Numerical results show that proportional time allocation provides better estimation performance as compared to equal time allocation.

ÖZET

TELSİZ DUYARGA AĞLARDA HEDEF TAKİBİ İÇİN KAYNAK DUYARLI UYARLANIR NİCEMLEME TASARIMI

Bu tezde, hareketli bir hedefin takibi için bir Telsiz Duyarga Ağı (TDA)'nda kaynak duyarlı uyarlanır nicemleme tasarlanmıştır. Düğüm enerjisi ya da haberleşme bant genişliği gibi kısıtlı kaynaklar nedeniyle duyargalar analog iletim yapmak yerine, öncelikle ölçümlerini ön işlemde geçirirler ve sonra da ikili nicemlenmiş biçimlerini ya doğrudan (tek-atlamalı iletim) ya da küme başı elemanları yardımıyla (iki-atlamalı iletim) son istatistiksel çıkarım için Tümlleştirme Merkezi (TM)'ne göndermektedirler. İlk olarak duyargaların yerel karar eşikleri, her hedef takibi adımında tanımlanan Çok-amaçlı Eniyileme Problemi (ÇEP) sayesinde eniyi ve devingen bir şekilde elde edilmektedir. Dikkate alınan ÇEP yöntemi kestirim hatasını ve merkeze veri gönderen duyarga sayısını tek-atlamalı bağlantılar altında müşterek olarak azaltmaktadır. İkinci olarak, ÇEP yöntemi aynı zamanda veri iletimi sırasında duyarga devrelerinde oluşan enerji tüketimi dikkate alınarak TDA'daki toplam enerji tüketimini tek-atlamalı ve 2-atlamalı bağlantılar altında en aza indirmek için de formüle edilmiştir. ÇEP'in yanı sıra duyarga ölçümlerinin en az enerji gerektiren bağlantı yolunu, tek-atlamalı ya da 2-atlamalı, takip ederek TM'ye ulaşmasını sağlayan En düşük İletim Enerjisi Yolu tabanlı veri iletimi tercih edilmektedir. Sayısal sonuçlar eniyiye yakın takip başarımı sağlamakla birlikte hem TDA'da harcanan toplam enerji oranında hem de veri iletimi yapan duyarga sayısında önemli ölçüde tasarruf edildiğini göstermektedir. Son olarak, kablosuz kanaldaki bozulmalar dikkate alınarak tek-atlamalı kanallar altında her bir duyargaya ikili kararlarını TM'ye iletmesi için tahsis edilen sürenin kendi ölçümü ile orantılı olduğu oransal Zaman Bölmeli Çoklu Erişim tabanlı MAC yaklaşımı önerilmektedir. Benzetim sonuçları, duyargalara oransal zaman tahsisi sağlanmasının, eşit zaman tahsisine göre daha iyi kestirim başarımı sağladığını göstermektedir.

TABLE OF CONTENTS

ACKNOWLEDGEMENTS	iii
ABSTRACT	iv
ÖZET	v
LIST OF FIGURES	viii
LIST OF TABLES	xi
LIST OF SYMBOLS/ABBREVIATIONS	xii
1. INTRODUCTION	1
1.1. LITERATURE SURVEY	3
1.2. LIST OF CONTRIBUTIONS	5
1.3. THESIS ORGANISATION	6
2. BACKGROUND	8
2.1. TARGET TRACKING PROBLEM	8
2.1.1. System Model	8
2.1.2. Generation of Sensor Decisions	10
2.2. PARTICLE FILTERING	11
2.3. INFORMATION METRICS FOR BINARY QUANTIZER DESIGN	12
2.3.1. Mutual Information	12
2.3.2. Fisher Information	14
2.4. MULTIOBJECTIVE OPTIMIZATION	17
2.4.1. NBI	18
2.4.2. NSGA-II	19
3. ADAPTIVE BINARY QUANTIZER DESIGN WITH MOP	22
3.1. FUSION OF SENSOR DECISIONS UNDER IDEAL CHANNELS	22
3.2. OBJECTIVE FUNCTIONS	23
3.2.1. Objective Function 1: Trace of FIM	24
3.2.2. Objective Function 2: Sum of Sensor Transmission Probabilities	24
3.3. NUMERICAL RESULTS	26
3.4. DISCUSSIONS	29
4. ENERGY AWARE DATA TRANSMISSION OF SENSOR DECISIONS	31
4.1. SELECTION OF DATA TRANSMISSION PATH	32

4.1.1.	Data Transmission under Single-hop Links.....	32
4.1.2.	Data Transmission under 2-hop Links.....	33
4.1.3.	MTEP based Data Transmission	35
4.1.4.	Numerical Results	36
4.2.	SENSOR DECISIONS WITH MOP UNDER MTEP	40
4.2.1.	Objective Functions.....	40
4.2.1.1.	Objective Function 1: Trace of FIM.....	41
4.2.1.2.	Objective Function 2: Total energy consumption in WSN	41
4.2.1.3.	Energy Consumption under MTEP with MOP	41
4.2.1.4.	Energy Consumption under Single-hop Links with MOP.....	43
4.2.2.	Numerical Results	43
4.3.	DISCUSSIONS	47
5.	TDMA BASED MAC SCHEME FOR TRANSMISSION OF DECISION UNDER FADING CHANNELS	48
5.1.	MEDIUM ACCESS MODEL.....	48
5.2.	WIRELESS CHANNEL EFFECTS.....	49
5.3.	FUSION OF SENSOR DECISIONS UNDER FADING CHANNELS	51
5.4.	OPTIMIZATION OF SENSOR DECISION THRESHOLDS.....	52
5.5.	NUMERICAL RESULTS	55
5.6.	PROPORTIONAL TIME ALLOCATION	58
5.6.1.	PTA maximizing the upperbound on Mutual Information.....	58
5.6.2.	PTA with respect to individual Mutual Information	59
5.6.3.	Numerical Results	59
6.	CONCLUSION AND FUTURE RESEARCH DIRECTIONS	63
	REFERENCES	65
	APPENDIX A	71
	APPENDIX B	73

LIST OF FIGURES

Figure 2.1.	An example of target trajectory and sensor deployments, $N=9$ sensors	9
Figure 2.2.	The point P is the solution of the single-objective constrained NBI subproblem outlined with the dashed line v	19
Figure 2.3.	A framework of NSGA-II algorithm.....	20
Figure 2.4.	Obtaining Pareto optimal front by NSGA-II	21
Figure 3.1.	Pareto optimal front obtained with NBI and NSGA-II at time step $t = 1$. For NSGA-II we used population size 200, crossover parameter 5, mutation parameter 5, and the Pareto-optimal front is shown after 100 generations.	26
Figure 3.2.	MSE at each time step of tracking.....	27
Figure 3.3.	Average number of sensors transmitting to the Fusion Center at each time step of tracking.....	28
Figure 3.4.	Sensor Decision Thresholds at the $t = 8^{th}$ time step of tracking (a) Solution 1, (b) Solution 2	30
Figure 4.1.	Transmission path in 2-hop and Single-hop	32
Figure 4.2.	Energy consumption steps during single-hop transmission	33
Figure 4.3.	Energy consumption steps during 2-hop transmission.....	34

Figure 4.4. A WSN example with 4 clusters (N=100 randomly deployed sensors)	35
Figure 4.5. Total energy consumption of network at each second with varying CHs ...	37
Figure 4.6. Energy consumption of each sensor in both three cases with fixed CHs (1: MTEP, 2: 2-hop, 3: Single-hop).....	38
Figure 4.7. Energy consumption of each sensor under Single-hop transmission	39
Figure 4.8. Energy consumption of each sensor under 2-hop transmission with fixed CHs.....	39
Figure 4.9. Energy consumption of each sensor under MTEP for fixed CHs.....	40
Figure 4.10. MTEP transmission tree (Red arrows:1 st hop, Blue arrows:2 nd hop (N=25))	42
Figure 4.11. Pareto optimal front under Single-hop and 2-hop.....	44
Figure 4.12. MSE at each time step of tracking.....	45
Figure 4.13. Average number of sensors transmitting to FC at each time step of tracking	45
Figure 4.14. Total energy consumption in WSN.....	46
Figure 5.1. Time Division Multiple Access	48
Figure 5.2. Target tracking performance of information metrics under ideal channels, $N = 9$	57
Figure 5.3. Target tracking performance of information metrics fading channels, $N = 9$.	57

Figure 5.4. Performance Comparison between ETA and PTA, $N = 9$ 60

Figure 5.5. Performance Comparison between ETA and PTA, $N = 16$ 61

Figure 5.6. Performance of ETA and PTA with sensor selection..... 62



LIST OF TABLES

Table 5.1. Simulation parameters	56
Table 5.2. Execution time to obtain optimum sensor thresholds comparison	56
Table 5.3. Probabilities of the received binary decisions and PTA values of each nodes at one step of tracking.....	60



LIST OF SYMBOLS/ABBREVIATIONS

A	Signal Gain
D_t	Transmit Sensor Decision
F	State Dynamics
H	Entropy
I	Mutual Information
P_0	Signal Power of The Target
P_R	Received Power
P_T	Transmit Power
R_t	Received Sensor Decision
Q	Covariance Matrix
η	Vector of Sensor Decision Thresholds
Δ	Target Sampling Interval
n	Measurement Noise
ρ	Process Noise Parameter
σ^2	Noise Variance
\mathbf{v}_t	Process Noise
x_t, y_t	Target Locations
\dot{x}_t, \dot{y}_t	Target Velocities
z	Received Signal at Sensor
AWGN	Additive White Gaussian Noise
CHIM	Convex Hull Of Individual Minima
C-PCRLB	Conditional Posterior Cramer Rao Lower Bound
ETA	Equal Time Allocation
$E_{circuit}$	Circuit Energy Consumption
FC	Fusion center
FI	Fisher Information

FIM	Fisher Information Matrix
LEACH	Low-Energy Adaptive Clustering Hierarchy
MAC	Medium Access Control
MI	Mutual Information
MMSE	Minimum Mean Square Error
MOP	Multiobjective Optimization Problem
MSE	Mean Squared Error
MTEP	Minimum Transmission Energy Path
NBI	Normal Boundary Intersection
NSGA-II	Non-dominated Sort Genetic Algorithm-II
PDF	Probability Density Function
PTA	Proportional Time Allocation
SIR	Sequential Importance Resampling
TDMA	Time Division Multiple Access
$\text{Tr}\{\mathbf{J}\}$	Trace of Fisher Information Matrix
WSNs	Wireless Sensor Networks

1. INTRODUCTION

A wireless sensor network (WSN) is composed of a number of spatially distributed sensors and a central node called fusion center, and when properly programmed and networked, a WSN is very useful in diverse application areas such as battlefield surveillance, industrial process or health monitoring and control [1]. Since a sensor is a tiny, battery powered device, the resources of the WSN is also limited. Therefore, adaptive sensor management strategies for WSNs determine the optimal way to manage available resources and task a group of sensors to collect measurements for statistical inference. Adaptive sensor management covers topics such as sensor selection, resource allocation, sensor placements. For instance, in a given region of interest dense deployment of sensors brings redundancy in coverage, sensor selection problem finds a subset of sensors to transmit to the fusion center and the remaining sensors stay silent while minimizing the error in estimation [2]. Similarly, dedicating the available WSN resources such as total transmission energy or transmission bandwidth to a subset of informative sensors may still provide the desired estimation performance [3].

In a WSN, the transmission of raw sensor measurements to the fusion center brings excessive energy and bandwidth consumption. Instead, for detection and estimation applications, the sensor measurements are first preprocessed by taking advantage of sensors limited onboard signal processing capabilities, and a quantized version of the measurements are sent to the fusion center. Adaptive sensor management considers joint optimization of multiple conflicting system objectives, such as minimizing the error on inference, minimizing the total energy consumption of the network, maximizing the lifetime of the network etc. With sensors censoring, only sensors with informative observation transmit to the fusion center [4] where local sensors employ binary on-off signalling. Then local sensor quantization thresholds not only determine the detection error probability or error in estimation, but also determine the number of sensors transmitting to the fusion center.

Since sensors in WSN have limited energy resources, excessive energy consumption need to be mitigated to enhance durability of network. One of the most challenging topic is to decide which path sensor nodes should use to forward information they collect. In contrast

to conventional transmissions, single-hop and multi-hop, cluster based data transmission is more energy efficient for life time of networks, because sensors which are far away from the base station in direct (single-hop) transmission die out quickly due to high path losses. In multi-hop, however, those are nearest to base station run out a few time after due to that they have to forward too much data to destination node. Thus, selecting minimum required energy path for transmission of sensors' decisions to destination node become more critical for life time of WSNs.

On the other hand, since sensors share the same medium, an appropriate medium access control (MAC) policy needs to be defined [5, 6]. Accordingly, scheduling sensors for state estimation is an important research topic [7–10]. Different from the MAC protocols designed for wireless networks which focus on efficient data delivery, WSN MAC protocols should also consider energy efficiency by maximizing the individual sensor or sensor network lifetime, or minimizing the communication in the WSN [5, 6]. As an example, time division multiple access (TDMA) based (MAC) strategies for WSNs allocate certain transmission time slots for sensor transmissions [8].

In this thesis, we propose a resource efficient target tracking based on binary quantized data and particle filtering in WSNs. Firstly, we solve an adaptive binary quantizer design problem where the local decision thresholds of sensors are obtained optimally and dynamically at each time step of tracking as a result from a Multiobjective Optimization Problem (MOP). Secondly, total energy consumption of WSN are further reduced by using MOP in our proposed deciding minimum transmission energy path while sensor are transmitting to fusion center to mitigate the drawbacks of single-hop and multi-hop transmission. Finally, we also proposed a TDMA based proportional time allocation method where more time is devoted to informative sensors to decrease their transmission errors at each time step of tracking by considering fading and noise channel effects. We first obtain the local sensor decision thresholds by maximizing Mutual Information (MI) and Fisher Information (FI) and then determine time allocation for each sensor based on information metrics. Overall, limited resources of a WSN such as energy, communication bandwidth and number of transmitting sensors are significantly reduced under different scenarios while maintaining a good estimation performance for target tracking.

1.1. LITERATURE SURVEY

Due to stringent resources such as energy and communication bandwidth, sensor measurements need to be first locally quantized before transmitted to the fusion center. For target localization, several quantization strategies have been proposed in [11]. For one-step ahead sensor management in target tracking, the local decision thresholds of sensors are updated optimally and dynamically at each time step of tracking where sensors transmit binary decisions to the fusion center [12], [13]. Furthermore, for multi-steps ahead sensor management, adaptive local quantizer design have been proposed in [14]. It is shown in [12], [13] that if the target is near a particular sensor, the sensing region of the sensor is decreased by increasing its decision threshold. Similarly, if a sensor is far away from the target, the sensing region of a sensor is increased by decreasing the decision threshold. On the other hand, the sensors far away from the target may carry negligible information about the target location, and due to reduced sensing threshold, the sensors may become sensitive to noise perturbations [15].

Design metrics for adaptive sensor management strategies, such as binary quantizer design and sensor selection, evolve either from information theory or estimation theory. One popular strategy for sensor selection is to use information driven methods [16], [17], [18], [19] where the main idea is to assign the network resources to the sensors which provide the most useful information quantified by entropy or MI. Conditional posterior Cramr-Rao lower bound based metrics, on the other hand, assigns the network resources to the sensors which minimize the error in estimation [20], [21], [22], [23]. As shown in [24], for sensor selection, the complexity to compute the MI increases exponentially with the number of sensors to be selected, whereas the computational complexity of FI, which is the inverse of the PCRLB, increases linearly with the number of sensors to be selected.

In the all aforementioned works, single-hop transmissions are considered between sensors and FC. Since sensors in WSN have limited energy resources, single-hop may not be an energy efficient for large scale networks in which very large path losses are likely to occur [25], [26], [27]. In [28], the M-bit quantized sensor measurements are transmitted over multi-hop relay fading channels where circuit energy is neglected. Estimation performance for target

tracking are determined under multi-hop relay fading channels. In [29], on the other hand, it is stated that when energy consumption in transmitter and receiver circuits of relay nodes are taken into account during transmissions, single-hop transmission would become more energy efficient than multi-hop unless path loss suppresses energy consumption of circuit electronics in relay nodes. Nevertheless, a cluster based energy-efficient communication protocol LEACH (Low-Energy Adaptive Clustering Hierarchy) for micro sensor networks are proposed in [25] where sensors are divided into different clusters that each cluster has a cluster head. Cluster heads which are selected adaptively according to energy level of sensors are responsible for forwarding sensors data to the base station.

In the above literature, it has been assumed that the transmission channels between sensors and fusion center are error-free. On the other hand, the channels between sensors and the fusion center may be non-reliable as a result of channel noise and fading. For the distributed detection in a WSN, the problem of obtaining optimal quantization rules has been reformulated by incorporating the channel impairments in [30], [31]. Furthermore, the optimal fusion rules under received sensor measurements subject to the channel fading have been presented in [32], and [4]. Given full and partial channel knowledge, [32] compares the detection performance of the optimal and sub-optimal fusion rules where sensors employ polar $\{-1, 1\}$ signalling. Considering sensor censoring where sensors transmit on-off signals $\{0, 1\}$, [4] formulates the optimal fusion rules using the statistics of the channels between sensors and the fusion center. The wireless channel models presented in [32] and [4] are then used in target localization [33] and target tracking [34].

Since sensors share the same medium, an appropriate medium access control (MAC) policy needs to be defined [5, 6]. MAC policies for WSNs fall into two categories as contention based and non-contention based policies. For the contention based MAC policies, the sensors first sense the medium, if the channel is idle, they then transmit their measurements. Since simultaneous sensor transmissions may cause collisions, collision avoidance routines and negotiation between sensors may be required. Such additional signalling may increase the energy consumption of individual sensors. For the non-contention based MAC policies, time division multiple access (TDMA) based multiple access strategies allocate certain transmission slots for sensor transmissions [8]. Since the number of time slots are limited, the scalability of

the MAC protocol is limited. To extend TDMA based MAC policies for a multi-hop WSNs, different sensors can access to the same time slot under the specified interference limits of each other [35]. TDMA is collision free but it requires clock synchronization between sensors and the central unit [8].

In terms of statistical inference problems, such as localization and tracking, the work presented in [9] consider a TDMA based sensor scheduling policy where at each time step of tracking, only one sensor transmit to the central controller. The sensors can be scheduled in a periodic manner or in a aperiodic manner. In the former case, the optimal transmission pattern needs to be determined, where in the later case the optimal sensor needs to be selected for transmission at each time step of tracking. Also for target tracking, in [8], the authors propose a distributed TDMA scheduling algorithm which consider the slot assignment problem. Finally, in [10], the authors consider a MAC protocol where the individual sensor measurements are summed up in the transmission medium and the central node observes the summation of the sensor measurements. In this scenario, in a dense network, only limited number of sensors contribute to the aggregate signal, and therefore the aggregate signal becomes sparse. Target tracking is then performed by using compressed sensing.

1.2. LIST OF CONTRIBUTIONS

In this thesis, resource efficient target tracking in WSNs are investigated. We develop novel adaptive sensor managements schemes which can noticeably save resources in terms of communication bandwidth, number of transmitting sensors used and energy consumption while maintaining a good tracking performance. Our contributions are listed as below,

- Adaptive binary quantizer design problem is solved for target tracking by using MOP under single-hop and 2-hop transmission. Simulation results show that solutions obtained by using MOP provides good target tracking performance while significantly reducing the average number of sensors transmitting to the fusion center at each time step of tracking.
- Instead of using only single-hop links or 2-hop links, we preferred a system that decide minimum transmission energy path to transmitting sensor decisions. We also apply

MOP to reduce energy burden on cluster heads during 2-hop transmission. By deciding MTEP, we observe that total energy consumption of network during transmission are become less than transmission under both single-hop and 2-hop links.

- TDMA based proportional time allocation are proposed for transmission of sensors' observations while considering impairments of the wireless channel. As a result, proportional time allocation among sensors where informative sensors possess more time for transmission provide better estimation performance as compared to equal time allocation.
- Overall, efficient resource managements are performed for target tracking with 1-bit quantized data under single-hop and 2-hops links while ensuring less energy consumption and communication traffic.

1.3. THESIS ORGANISATION

The rest of the thesis is organized as follows,

In Chapter 2, we introduce the fundamentals of background information to be used in following chapters. Firstly, we present target tracking problem which introduce system model and generation of sensor decisions. Secondly, we explain the particle filtering methods which is used to state parameters estimation for target tracking problem. In addition, derivation of information metrics are given under ideal channels which we used for deciding sensor decision thresholds and allocated times. Finally, we review multiobjective optimization approach with NBI and NSGA-II methods.

In Chapter 3, adaptive binary quantizer design problem is solved by minimizing estimation error and reducing number of transmitting sensors using defining objective functions using MOP under single-hop links assuming ideal channel. In addition, we present simulation results which compare estimation performance and number of transmitting sensors based on sensor decision thresholds obtained by maximizing trace of fisher information and MOP.

In Chapter 4, we determine energy consumption of overall network sensors under single-hop and 2-hop links. We decide minimum transmission energy path for transmitting sensor

decisions by comparing required energy under single-hop and 2-hop transmissions while considering energy consumption in hardware of sensor circuits. Furthermore, we also combine MOP with the MTEP to reduce overload energy consumption on cluster head nodes.

In Chapter 5, we study on medium access model and time division multiple access for scheduling sensors for target tracking. We proposed proportional time allocation methods where the simulation results compare the performance of proportional time sharing with equal time sharing when different number of sensors compete for time allocations. In contrast to other chapters, optimal and suboptimal metrics are compared based on estimation performance while considering wireless channel impairments.

In Chapter 6, we give a summary of the basic results of the thesis and mention some suggestions with future directions.

2. BACKGROUND

In this chapter, we basically summarize the necessary background for several topics that will be considered in the thesis. Since we deal with tracking in wireless sensor networks, we first present the mathematical modeling of system model under target tracking problem and Monte-Carlo based particle filtering method. Secondly, we mention the information metrics such as mutual information and fisher information. Finally we briefly review problem formulation of multiobjective optimization and NBI method.

2.1. TARGET TRACKING PROBLEM

In recent years, tracking moving objects in WSNs become an attractive research area [36], [37]. Due to dynamic nature of moving targets, tracking problem requires dynamic resource allocation at each time step of tracking. In Figure 2.1, an example of target trajectory are given with sensor deployments. In thesis, we use different number of sensors depend on proposed networks. In this chapter, we introduce model parameters for target tracking and assign decisions based on sensor observations.

2.1.1. System Model

At time step t , we define the target by a 4-dimensional state vector $\mathbf{x}_t \triangleq [x_t \ y_t \ \dot{x}_t \ \dot{y}_t]^T$ where x_t and y_t are the target location at discrete time steps t , \dot{x}_t and \dot{y}_t are the target velocities in x and y directions respectively. Then according to the white noise acceleration model \mathbf{x}_{t+1} is obtained as,

$$\mathbf{x}_{t+1} = \mathbf{F}\mathbf{x}_t + \mathbf{v}_t \quad (2.1)$$

where Δ is the target sampling interval, \mathbf{F} models the state dynamics and \mathbf{v}_t is the process noise, which is assumed to be white, zero-mean and Gaussian with the covariance matrix \mathbf{Q} .

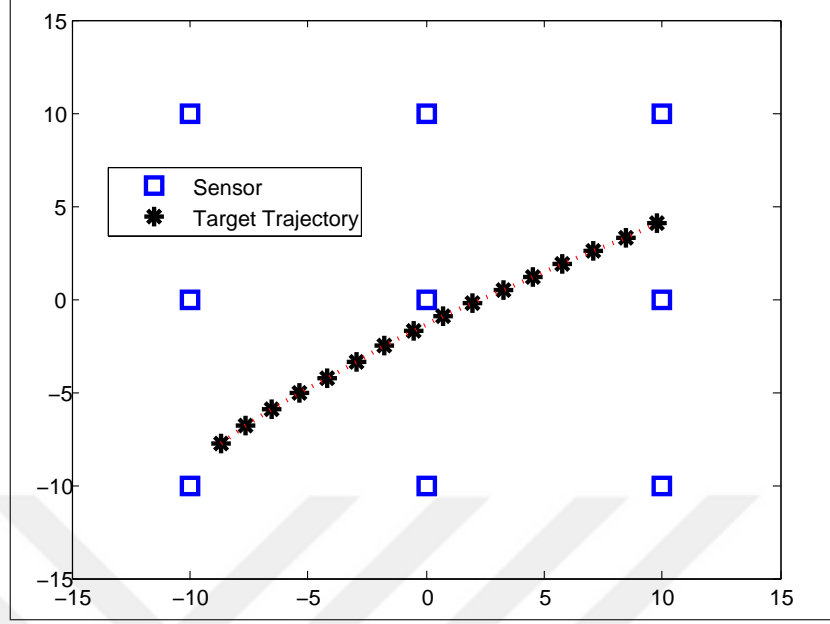


Figure 2.1. An example of target trajectory and sensor deployments, $N=9$ sensors

\mathbf{F} and \mathbf{Q} are represented as,

$$\mathbf{F} \triangleq \begin{bmatrix} 1 & 0 & \Delta & 0 \\ 0 & 1 & 0 & \Delta \\ 0 & 0 & 1 & 0 \\ 0 & 0 & 0 & 1 \end{bmatrix}, \quad \mathbf{Q} \triangleq \rho \begin{bmatrix} \frac{\Delta^3}{3} & 0 & \frac{\Delta^2}{2} & 0 \\ 0 & \frac{\Delta^3}{3} & 0 & \frac{\Delta^2}{2} \\ \frac{\Delta^2}{2} & 0 & \Delta & 0 \\ 0 & \frac{\Delta^2}{2} & 0 & \Delta \end{bmatrix} \quad (2.2)$$

where ρ denotes the process noise parameter. We assume that the fusion center has perfect information about the target state-space model in (2.1).

The target is assumed to be an acoustic or an electromagnetic source that follows the power attenuation model given in [38]. At any time step t , the signal power received at sensor i is expressed as,

$$a_{i,t}^2 = \frac{P_0}{1 + d_{i,t}^\alpha} \quad (2.3)$$

where P_0 denotes the signal power of the target, α is the signal decay exponent. $d_{i,t}$ is the

distance between the target and the i^{th} sensor, $d_{i,t} = \sqrt{(x_i - x_t)^2 + (y_i - y_t)^2}$, where (x_i, y_i) are the coordinates of the i^{th} sensor. Without loss of generality, in this part, we select $\alpha = 2$. At time step t , the received signal at sensor i is given by

$$z_{i,t} = a_{i,t} + n_{i,t} \quad (2.4)$$

where $n_{i,t}$ is the measurement noise term modeled as additive white Gaussian noise (AWGN), i.e., $n_{i,t} \sim \mathcal{N}(0, \sigma^2)$, which represents the cumulative effects of sensor background noise and the modeling error of signal parameters.

2.1.2. Generation of Sensor Decisions

A sensor measurement $z_{i,t}$ at sensor i is locally binary quantized before its transmission to the fusion center. Let $D_{i,t}$ be the 1-bit observation of sensor i at time step t , then

$$D_{i,t} = \begin{cases} 0 & -\infty < z_{i,t} < \eta_{i,t} \\ 1 & \eta_{i,t} < z_{i,t} < \infty \end{cases} \quad (2.5)$$

$\boldsymbol{\eta}_t \triangleq [\eta_{1,t} \ \eta_{2,t} \ \dots \ \eta_{N,t}]$ represents the vector of sensor decision thresholds at time step t . Given \mathbf{x}_t , it is easy to show that the probability of quantization output 1 is,

$$P(D_{i,t} = 1 | \mathbf{x}_t) = Q\left(\frac{\eta_{i,t} - a_{i,t}}{\sigma}\right) \quad (2.6)$$

where $Q(\cdot)$ is the complementary distribution function of the standard Gaussian distribution with zero mean and unit variance,

$$Q(x) = \int_x^\infty \frac{1}{\sqrt{2\pi}} \exp\left(-\frac{t^2}{2}\right) dt \quad (2.7)$$

2.2. PARTICLE FILTERING

Accurate estimation of the state of a system that changes over time using a sequence of noisy measurements made on the system is required to handle a target tracking problem. Kalman filter solves Bayesian sequential estimation problem for linear and Gaussian systems. Also the extended Kalman filter fails for nonlinear systems when the sensor measurements are quantized [1]. However, the particle-filtering techniques appear quite appropriate for dealing with this kind of problem. Particle filtering is a general Monte Carlo (sampling) method for performing inference in state space models where the state of a system evolves in time and information about the state is obtained via noisy measurements made at each time step [2].

Let $D_{i,t}$ the 1-bit observation of sensor i at time step t , as the received sensors measurements at time t . We can find the discrete representation of the posterior distribution $p(\mathbf{x}_{t+1}|\mathbf{D}_{i,t})$ using a set of particles \mathbf{x}_t^s with related weights $w^s \{s = 1, 2, \dots, N_s\}$. The posterior distribution function at time t can be written approximately as,

$$p(\mathbf{x}_{t+1}|\mathbf{D}_{i,t}) \approx \sum_{s=1}^{N_s} w^s \delta(\mathbf{x}_{t+1} - \mathbf{x}_{t+1}^s) \quad (2.8)$$

The weight w_{t+1}^s of particle \mathbf{x}_{t+1}^s can be obtained as,

$$w_{t+1}^s \approx p(\mathbf{D}_{i,t}|\mathbf{x}_{t+1}^s) \quad (2.9)$$

The particle weights are normalized as,

$$w_{t+1}^s = \frac{w_{t+1}^s}{\sum_{j=1}^{N_s} w_{t+1}^j} \quad (2.10)$$

At the end, the state estimation of target at time step $t + 1$ is given as,

$$\hat{\mathbf{x}}_{t+1} = \sum_{s=1}^{N_s} w_{t+1}^s \mathbf{x}_{t+1}^s \quad (2.11)$$

2.3. INFORMATION METRICS FOR BINARY QUANTIZER DESIGN

In this section, we review the metrics to determine the decision thresholds of local sensors. In this section, we present information theoretic and estimation theoretic metrics and their approximations for binary quantizer design. In this part, derivations of information metrics are only based on ideal channels in which transmitted quantized sensor measurements \mathbf{D}_{t+1} are taken as same at fusion center. We find derivations of information metrics in Chapter 5 for considering impairments of the wireless channel.

2.3.1. Mutual Information

At each time step of tracking, fusion center determines the vector of sensor decision thresholds $\boldsymbol{\eta}_{t+1}$ which maximize the mutual information for the next time step of tracking $I(\mathbf{x}_{t+1}, \mathbf{D}_{t+1})$ between the received sensor decisions, and the location of the target. The mutual information is computed from,

$$I(\mathbf{x}_{t+1}, \mathbf{D}_{t+1}) = H(\mathbf{D}_{t+1}) - H(\mathbf{D}_{t+1}|\mathbf{x}_{t+1}) \quad (2.12)$$

where $H(\mathbf{D}_{t+1})$ is the entropy of \mathbf{D}_{t+1} and $H(\mathbf{D}_{t+1}|\mathbf{x}_{t+1})$ is the conditional entropy of \mathbf{D}_{t+1} given the target location \mathbf{x}_{t+1} . Firstly, $H(\mathbf{D}_{t+1})$ is computed from,

$$\begin{aligned} H(\mathbf{D}_{t+1}) &= - \sum_{\mathbf{D}_{t+1}} P(\mathbf{D}_{t+1}) \log_2 P(\mathbf{D}_{t+1}) \\ &= - \sum_{d_1=0}^1 \dots \sum_{d_N=0}^1 P(D_{1,t+1} = d_1, \dots, D_{N,t+1} = d_N) \\ &\quad \times \log_2 P(D_{1,t+1} = d_1, \dots, D_{N,t+1} = d_N) \end{aligned} \quad (2.13)$$

where

$$\begin{aligned}
& P(D_{1,t+1} = d_1, \dots, D_{N,t+1} = d_N) \\
&= \int P(D_{1,t+1} = d_1, \dots, D_{N,t+1} = d_N | \mathbf{x}_{t+1}) p(\mathbf{x}_{t+1}) d\mathbf{x}_{t+1} \\
&= \int \left(\prod_{i=1}^N P(D_{i,t+1} = d_i | \mathbf{x}_{t+1}) \right) p(\mathbf{x}_{t+1}) d\mathbf{x}_{t+1} \tag{2.14}
\end{aligned}$$

Using the particle filter approximation of $p(\mathbf{x}_{t+1}) \approx p(\mathbf{x}_{t+1} | \mathbf{D}_t)$, $P(D_{1,t+1} = d_1, \dots, D_{N,t+1} = d_N)$ is approximated by

$$\begin{aligned}
& P(D_{1,t+1} = d_1, \dots, D_{N,t+1} = d_N) \approx \sum_{s=1}^{N_s} w_{t+1}^s \\
& \times \left[\prod_{i=1}^N \left(\sum_{d_i=0}^1 P(D_{i,t+1} = d_i) P(D_{i,t+1} = d_i | \mathbf{x}_{t+1}^s) \right) \right] \tag{2.15}
\end{aligned}$$

Secondly, the conditional entropy $H(\mathbf{D}_{t+1}|\mathbf{x}_{t+1})$ is computed as,

$$\begin{aligned}
H(\mathbf{D}_{t+1}|\mathbf{x}_{t+1}) &= - \int_{\mathbf{x}_{t+1}} \sum_{\mathbf{D}_{t+1}} p(\mathbf{D}_{t+1}, \mathbf{x}_{t+1}) \log_2 p(\mathbf{D}_{t+1}|\mathbf{x}_{t+1}) d\mathbf{x}_{t+1} \\
&= - \int_{\mathbf{x}_{t+1}} \sum_{\mathbf{D}_{t+1}} [p(\mathbf{D}_{t+1}|\mathbf{x}_{t+1}) \log_2 p(\mathbf{D}_{t+1}|\mathbf{x}_{t+1})] p(\mathbf{x}_{t+1}) d\mathbf{x}_{t+1} \\
&= - \int_{\mathbf{x}_{t+1}} \sum_{d_1=0}^1 \cdots \sum_{d_N=0}^1 \left[\left(\prod_{i=1}^N P(D_{i,t+1} = d_i|\mathbf{x}_{t+1}) \right) \right. \\
&\quad \left. \log_2 \left(\prod_{i=1}^N P(D_{i,t+1} = d_i|\mathbf{x}_{t+1}) \right) \right] p(\mathbf{x}_{t+1}) d\mathbf{x}_{t+1} \\
&= - \int_{\mathbf{x}_{t+1}} \sum_{i=1}^N \sum_{d_i=0}^1 [P(D_{i,t+1} = d_i|\mathbf{x}_{t+1}) \log_2 P(D_{i,t+1} = d_i|\mathbf{x}_{t+1})] \\
&\quad p(\mathbf{x}_{t+1}) d\mathbf{x}_{t+1} \tag{2.16}
\end{aligned}$$

2.3.2. Fisher Information

For a Bayesian estimator, Posterior Cramer Rao Lower Bound (PCRLB) provides the theoretical performance limit. Let $p(\mathbf{D}_{t+1}, \mathbf{x}_{t+1})$ be the joint probability density of the received sensor data, \mathbf{D}_{t+1} , and the unknown state, \mathbf{x}_{t+1} , then we define $\hat{\mathbf{x}}_{t+1}$ is the estimate of \mathbf{x}_{t+1} based on \mathbf{D}_{t+1} for time step $t + 1$. Although the PCRLB is an off-line metric, since it is computed by averaging all the sensor measurements, Conditional PCRLB (C-PCRLB) is a very useful online sensor management metric, since it provides an error bound for the given sequence of sensor measurements [39]. In this thesis, by using sensor data received at time step t , \mathbf{D}_t , we utilize the Conditional FIM, which is the inverse of C-PCRLB, to determine the best sensor management strategy for time step $t + 1$. In other words, at time step t , we find the optimal way of allocating available resources to maximize the Conditional Fisher Information, \mathbf{J}_{t+1} . \mathbf{J}_{t+1} which has the form,

$$E \{ [\hat{\mathbf{x}}_{t+1} - \mathbf{x}_{t+1}] [\hat{\mathbf{x}}_{t+1} - \mathbf{x}_{t+1}]^T \} \geq \mathbf{J}_{t+1}^{-1} \quad (2.17)$$

where \mathbf{J}_{t+1} is the 4×4 Fisher information matrix (FIM) defined by,

$$\begin{aligned} \mathbf{J}_{t+1} &\triangleq E_{p(\mathbf{x}_{t+1}, \mathbf{D}_{t+1})} \left[-\nabla_{\mathbf{x}_{t+1}}^{\mathbf{x}_{t+1}} \log p(\mathbf{x}_{t+1}, \mathbf{D}_{t+1}) \right] \\ &= - \underbrace{\int_{\mathbf{x}_{t+1}} \sum_{\mathbf{D}_{t+1}} P(\mathbf{D}_{t+1} | \mathbf{x}_{t+1}) \left[-\nabla_{\mathbf{x}_{t+1}}^{\mathbf{x}_{t+1}} \log P(\mathbf{D}_{t+1} | \mathbf{x}_{t+1}) \right] p(\mathbf{x}_{t+1}) d\mathbf{x}_{t+1}}_{\triangleq \mathbf{J}_{t+1}^D} \\ &\quad - \underbrace{\int_{\mathbf{x}_{t+1}} \left[-\nabla_{\mathbf{x}_{t+1}}^{\mathbf{x}_{t+1}} \log p(\mathbf{x}_{t+1}) \right] p(\mathbf{x}_{t+1}) d\mathbf{x}_{t+1}}_{\triangleq \mathbf{J}_{t+1}^P} \end{aligned} \quad (2.18)$$

where \mathbf{J}_{t+1} can be decomposed into data part, \mathbf{J}_{t+1}^D and prior part, \mathbf{J}_{t+1}^P . Data part of the Fisher Information can be further written as,

$$\begin{aligned} \mathbf{J}_{t+1}^D &= - \int_{\mathbf{x}_{t+1}} \sum_{d_1=0}^1 \cdots \sum_{d_N=0}^1 \\ &\quad \left(\prod_{i=1}^N P(D_{i,t+1} = d_i | \mathbf{x}_{t+1}) \right) \left[-\nabla_{\mathbf{x}_{t+1}}^{\mathbf{x}_{t+1}} \log \left(\prod_{i=1}^N P(D_{i,t+1} = d_i | \mathbf{x}_{t+1}) \right) \right] p(\mathbf{x}_{t+1}) d\mathbf{x}_{t+1} \\ &= \sum_{i=1}^N \left\{ - \int_{\mathbf{x}_{t+1}} \sum_{d_i=0}^1 P(D_{i,t+1} = d_i | \mathbf{x}_{t+1}) \left[-\nabla_{\mathbf{x}_{t+1}}^{\mathbf{x}_{t+1}} \log P(D_{i,t+1} = d_i | \mathbf{x}_{t+1}) \right] \right. \\ &\quad \left. \times p(\mathbf{x}_{t+1}) d\mathbf{x}_{t+1} \right\} \end{aligned} \quad (2.19)$$

where \mathbf{J}_{t+1}^D is equal to sum of each sensors contribution to the Fisher Information, $\mathbf{J}_{i,t+1}^D$. Using the properties given in [11], $\mathbf{J}_{i,t+1}^D$ can be written as,

$$\begin{aligned} \mathbf{J}_{i,t+1}^D &= \int_{\mathbf{x}_{t+1}} \sum_{d_i=0}^1 \frac{1}{P(D_{i,t+1} = d_i | \mathbf{x}_{t+1})} \left(\frac{\partial}{\partial \mathbf{x}_{t+1}} P(D_{i,t+1} = d_i | \mathbf{x}_{t+1}) \right)^2 \\ &\quad \times p(\mathbf{x}_{t+1}) d\mathbf{x}_{t+1} \end{aligned} \quad (2.20)$$

where detailed derivation of $\frac{\partial}{\partial \mathbf{x}_{t+1}} P(D_{i,t+1} = d_i | \mathbf{x}_{t+1})$ is given in [3]. Using the particle filter approximation $\mathbf{J}_{i,t+1}^D$ is approximated by

$$\begin{aligned} \mathbf{J}_{i,t+1}^D &\approx \\ &\sum_{s=1}^{N_s} \frac{1}{N_s} \left\{ \sum_{d_i=0}^1 \frac{1}{P(D_{i,t+1} = d_i | \mathbf{x}_{t+1}^s)} \left(\frac{\partial}{\partial \mathbf{x}_{t+1}} P(D_{i,t+1} = d_i | \mathbf{x}_{t+1}^s) \right)^2 \right\} \end{aligned} \quad (2.21)$$

In summary, \mathbf{J}_{t+1} is written as,

$$\begin{aligned} \mathbf{J}_{t+1} &= \mathbf{J}_{t+1}^D + \mathbf{J}_{t+1}^P \\ &= \sum_{i=1}^N \mathbf{J}_{i,t+1}^D + \mathbf{J}_{t+1}^P \end{aligned} \quad (2.22)$$

Since we model $p(\mathbf{x}_{t+1} | \mathbf{D}_{1:t})$ by a set of particles with associated weights, it becomes very difficult to calculate the exact \mathbf{J}_{t+1}^P . Instead, we use a Gaussian approximation such that $p(\mathbf{x}_{t+1} | \mathbf{D}_{1:t}) \approx \mathcal{N}(\boldsymbol{\mu}_{t+1}, \boldsymbol{\Sigma}_{t+1})$, where

$$\boldsymbol{\mu}_{t+1} \triangleq \frac{1}{N_s} \sum_{s=1}^{N_s} \mathbf{x}_{t+1}^s \quad (2.23)$$

and

$$\boldsymbol{\Sigma}_{t+1} \triangleq \frac{1}{N_s} \sum_{s=1}^{N_s} (\mathbf{x}_{t+1}^s - \boldsymbol{\mu}_{t+1})(\mathbf{x}_{t+1}^s - \boldsymbol{\mu}_{t+1})^T \quad (2.24)$$

Given the Gaussian approximation, it is easy to show that $\mathbf{J}_{t+1}^P = (\boldsymbol{\Sigma}_{t+1})^{-1}$.

2.4. MULTIOBJECTIVE OPTIMIZATION

In this section, we first review the fundamentals of multiobjective optimization, then we summarize Normal Boundary Intersection (NBI) method to solve the multiobjective optimization problem. The mathematical description of a multiobjective optimization problem can be stated as follows:

$$\min_{\chi \in C} [f_1(\chi) \quad f_2(\chi) \quad \dots f_n(\chi)]^T \quad (2.25)$$

where χ is a solution to the MOP. The number of objectives $n \geq 2$ and the feasible set C ,

$$C : \{\chi : h(\chi) = 0, g(\chi) \leq 0, a \leq \chi \leq b\} \quad (2.26)$$

is subject to the equality and inequality constraints denoted as $h(\chi)$ and $g(\chi)$ respectively, and explicit variable bounds $[a, b]$. In a minimization problem, a solution χ_1 dominates another solution χ_2 ($\chi_1 \gg \chi_2$) if and only if

$$f_u(\chi_1) \leq f_u(\chi_2) \quad \forall u \in \{1, 2, \dots, n\}$$

$$f_v(\chi_1) < f_v(\chi_2) \quad \exists v \in \{1, 2, \dots, n\} \quad (2.27)$$

and a solution χ^* is the Pareto optimal solution for the MOP if and only if there is no $\chi \in C$ that dominates χ^* . Pareto optimal points are also known as non-dominated points. A well known technique for solving MOPs is to minimize a weighted sum of the objectives. As shown in [40], minimizing the weighted sum of the objectives suffers from several drawbacks. First of all, a uniform spread of weights rarely produces a uniform spread of points on the Pareto front. Some of the optimal design solutions are closely spaced, which reduce the number of design alternatives. Secondly, if the Pareto optimal curve is not a convex function, the Pareto points on the concave parts of the actual Pareto optimal curve will be missed.

Moreover, since it is up to the user to choose appropriate weights, decision on the preferences may not be clear to the user until the solution is generated.

2.4.1. NBI

The NBI is a computationally efficient method in locating the Pareto optimal points. The NBI method [41] reduces the MOP to multiple number of single-objective constrained problems, called NBI subproblems. This method starts with finding the optimizers of each objective function separately. For the two-objective example illustrated in Figure 2.4.1 [42], the shaded area represents the region of feasible design and the curve at the lower boundary is the Pareto optimal front. The convex hull of individual minima (CHIM) is defined as the line segment AB. Any NBI problem is then specified by a reference point on the CHIM such as the point H. Let χ_j^* be the minimizer of the j^{th} objective and $F_j^* = F(\chi_j^*) = [f_1(\chi_j^*) \dots f_n(\chi_j^*)]^T$, F^* is the shadow minimum which consists of individual minima of objectives, the payoff matrix Φ , is an $n \times n$ matrix whose j^{th} column is $F_j^* - F^*$. $\Phi\beta$ then denotes the reference point H, and each NBI subproblem is defined as,

$$\max_{\chi, \tau} \tau$$

$$\text{s.t. } \Phi\beta + \tau v = F(\chi)$$

$$h(\chi) = 0; g(\chi) \leq 0; a \leq \chi \leq b \quad (2.28)$$

The length of the line segment HP, τ , represents the new variable introduced by the NBI subproblem. The new constraint given the NBI subproblem ensures that the point lies inside the feasible set C . The number of NBI subproblems determines the resolution of the Pareto front. Clearly larger values for this parameter imply a better resolution of the Pareto front. If the Pareto set is disconnected, it is concluded that some of the subproblems have no solution [41]. Each NBI subproblem can be solved with any appropriate optimization method.

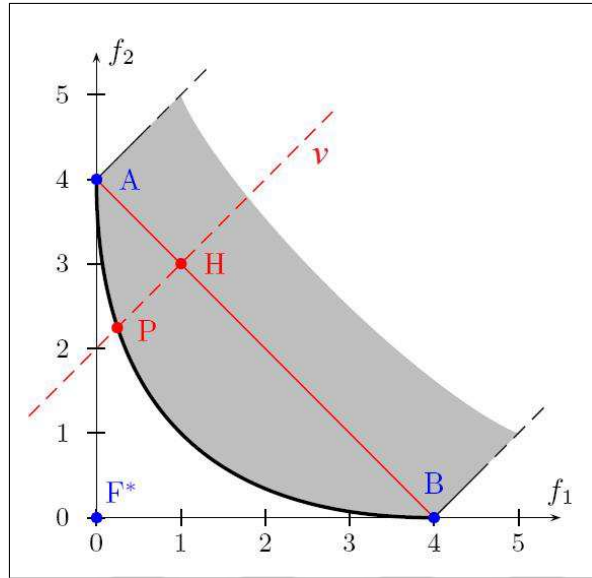


Figure 2.2. The point P is the solution of the single-objective constrained NBI subproblem outlined with the dashed line v

2.4.2. NSGA-II

Non-Dominating sorting genetic algorithm-II (NSGA-II) is an elitist multiobjective evolutionary algorithm which keep best individuals in the population. NSGA-II requires non-dominated solutions in each front and rate them according to their rank and crowding distance values [43].

As seen in Figure 2.3, parents P_t and offspring populations Q_t with size of N are represented as one population R_t which is sorted based on non-dominated sorting process. Non-dominated sorting find non-dominated fronts F sets. Solutions which are not dominated by any other solutions are assigned to first rank (or fitness). Dominated solutions are deleted from the populations until all non-dominated solutions have their rank level. For example, F_1 is best front. Then, best F sets are transferred to crowded comparison operator. Solutions are compared according to theirs rank and crowding distance values in crowded comparison operator part. Operator, firstly, prefer solution which has the lower rank. If the ranks of two solutions are same, algorithm select the solution that has higher crowding distance (distance between adjacent solutions). At the end, new populations of P_{t+1} are used to make new

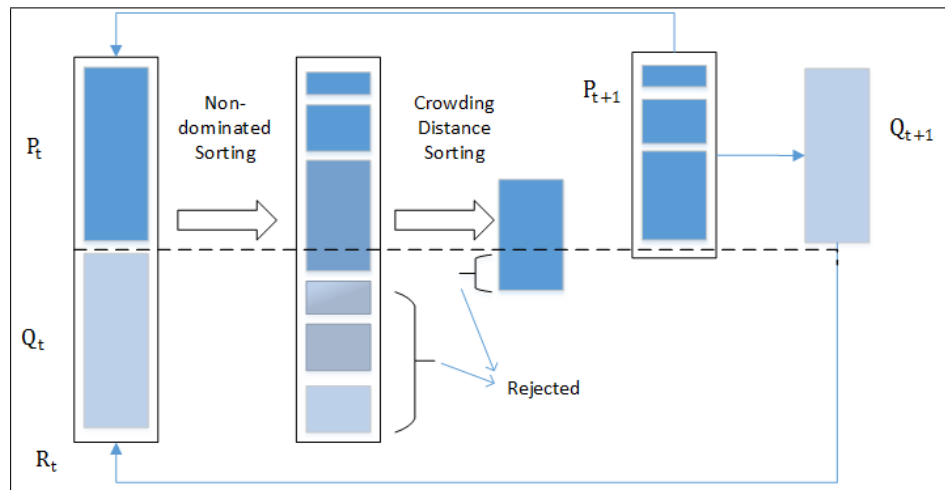


Figure 2.3. A framework of NSGA-II algorithm

generation of offsprings $Q_t + 1$ and the steps are repeated to find Pareto-optimal front as shown in Figure 2.4.

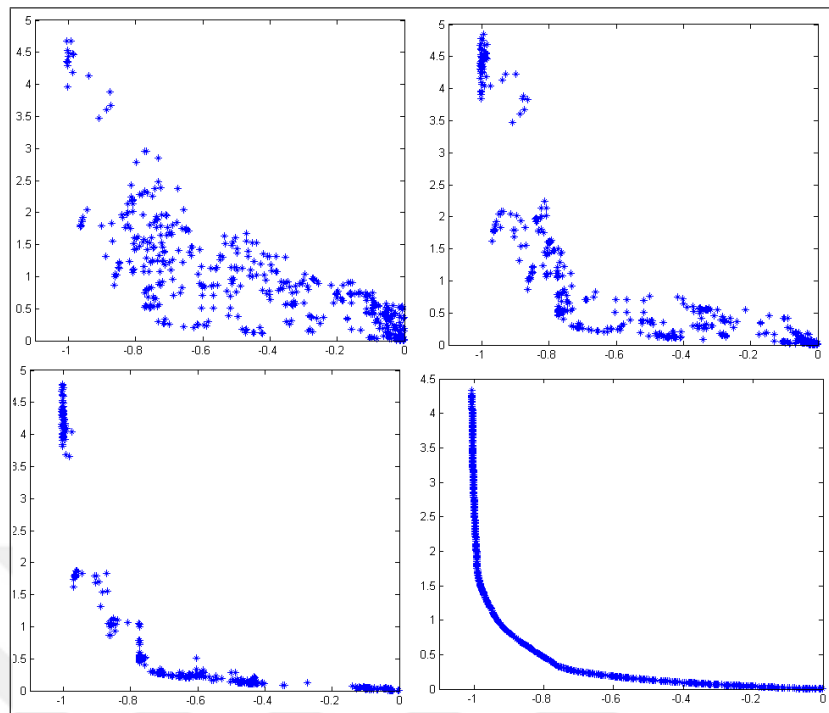


Figure 2.4. Obtaining Pareto optimal front by NSGA-II

3. ADAPTIVE BINARY QUANTIZER DESIGN WITH MOP

In this chapter, we solve the adaptive binary quantizer design problem in target tracking using multiobjective optimization. We jointly maximize the trace of the Fisher Information matrix for minimizing the error in estimation and minimize the sum of sensor transmission probabilities. We solve the multiobjective problem using NBI method and simulation results show that NBI provides computationally very efficient results as compared to NSGA-II with good tracking performance while significantly reducing the average number of transmitting sensors to the fusion center.

3.1. FUSION OF SENSOR DECISIONS UNDER IDEAL CHANNELS

Let the fusion center receive the data vector $\mathbf{D}_t = [D_{1,t}, \dots, D_{N,t}]$ from the N sensors, then

$$p(\mathbf{D}_t|\mathbf{x}_t) = \prod_{i=1}^N p(D_{i,t}|\mathbf{x}_t) \quad (3.1)$$

Based on the received sensor decisions, the MMSE estimate of the target location is obtained as,

$$\hat{\mathbf{x}}_t = \int \mathbf{x}_t p(\mathbf{x}_t|\mathbf{D}_t) d\mathbf{x}_t \quad (3.2)$$

Here $p(\mathbf{x}_t|\mathbf{D}_t)$ represents the posterior PDF of the target location upon the reception of sensor decisions at time t . As a result of Bayes rule $p(\mathbf{x}_t|\mathbf{D}_t) \propto P(\mathbf{D}_t|\mathbf{x}_t)p(\mathbf{x}_t)$. $p(\mathbf{x}_t) \approx p(\mathbf{x}_t|\mathbf{D}_{t-1})$ is the prior probability of target location that is the probability distribution of \mathbf{x}_t upon the reception of sensor decisions \mathbf{D}_{t-1} . We compute Eqn. 3.2 numerically using the sequential importance resampling (SIR) based Particle Filtering method as described in Algorithm 3.1.

For tracking the target emitting energy, we use a sequential importance resampling (SIR) based Particle Filtering method as shown in Algorithm 3.1. For the propagation step of the algorithm, we determine the vector of decision thresholds $\boldsymbol{\eta}_t$ using Multiobjective optimization. After the

fusion center receives the binary sensor measurements from N sensors, the particle weights are updated and the target location is estimated for $t + 1$. Furthermore, resampling step avoids the situation that all but one of the importance weights are close to zero [44].

$$p(\mathbf{x}_t | \mathbf{D}_t) \approx \sum_{s=1}^{N_s} w_t^s \delta(\mathbf{x}_t - \mathbf{x}_t^s) \quad (3.3)$$

where N_s is the total number of particles, and $w_t^s = 1/N_s$. Then, \mathbf{x}_{t+1}^s 's are obtained by propagating \mathbf{x}_t^s using Eqn. 2.1 to obtain the prior

$$p(\mathbf{x}_{t+1} | \mathbf{D}_t) \approx \frac{1}{N_s} \sum_{s=1}^{N_s} \delta(\mathbf{x}_{t+1} - \mathbf{x}_{t+1}^s) \quad (3.4)$$

Algorithm 3.1. SIR based Particle Filtering with MOP for Target Tracking

Set $t = 0$. Generate initial particles $\mathbf{x}_0^s \sim p(\mathbf{x}_0)$ with $\forall s, w_0^s = N_s^{-1}$.

while $t \leq T_S$ **do**

Propagate particles $\mathbf{x}_{t+1}^s = \mathbf{F}\mathbf{x}_t^s + \mathbf{v}_t$ and $p(\mathbf{x}_{t+1} | \mathbf{D}_t) = \frac{1}{N_s} \sum_{s=1}^{N_s} \delta(\mathbf{x}_{t+1} - \mathbf{x}_{t+1}^s)$.

Decide sensor decision thresholds using Multiobjective Optimization.

Get binary sensor measurements, $w_{t+1}^s \propto p(\mathbf{D}_{t+1} | \mathbf{x}_{t+1}^s)$. (Updating weights)

$w_{t+1}^s = \frac{w_{t+1}^s}{\sum_{j=1}^{N_s} w_{t+1}^j}$. (Normalizing weights)

$\hat{\mathbf{x}}_{t+1} = \sum_{s=1}^{N_s} w_{t+1}^s \mathbf{x}_{t+1}^s$. (State estimation)

$\{\mathbf{x}_{t+1}^s, N_s^{-1}\} = \text{Resampling}(\mathbf{x}_{t+1}^s, w_{t+1}^s)$

$t = t + 1$

end while

3.2. OBJECTIVE FUNCTIONS

Here, we consider joint optimization of two objective functions. By considering the first objective function, we desire to reduce the estimation error in target tracking and by considering the second objective function, we desire to minimize the total number of sensors reporting to the fusion center. Note that the objective functions are conflicting where minimizing the total number of sensors reporting to the fusion center increases the estimation error.

3.2.1. Objective Function 1: Trace of FIM

Since C-PCRLB is the lower bound on the estimation error, minimizing the lower bound $\text{Tr}\{\mathbf{J}_{t+1}^{-1}\}$ also minimizes the error in estimation. Similarly, under Gaussian assumption, maximizing the determinant of the FIM, $\det(\mathbf{J}_{t+1})$, is equivalent to minimizing the volume of the uncertainty ellipsoid [45]. These two metrics are quite popular in sensor management problems. Furthermore, the inverse of $\text{Tr}\{\mathbf{J}_{t+1}\}$ is further a lower bound on $\text{Tr}\{\mathbf{J}_{t+1}^{-1}\}$ [46]. It is also shown in [14], [47] that maximizing $\text{Tr}\{\mathbf{J}_{t+1}\}$ maximizes the FIM in a positive definite sense. Despite maximizing $\text{Tr}\{\mathbf{J}_{t+1}\}$ yields suboptimality¹ relative to minimizing $\text{Tr}\{\mathbf{J}_{t+1}^{-1}\}$ or maximizing $\det(\mathbf{J}_{t+1})$, evaluation of $\text{Tr}\{\mathbf{J}_{t+1}\}$ significantly reduces the computation time of the objective function due to its simple form. Therefore, in this part, we maximize $\text{Tr}\{\mathbf{J}_{t+1}\}$ for sensor management as,

$$\begin{aligned} \min_{\boldsymbol{\eta}_{t+1}} f_1(\boldsymbol{\eta}_{t+1}) &= -\text{Tr}\{\mathbf{J}_{t+1}\} \\ &= -\sum_{i=1}^N \text{Tr}\{\mathbf{J}_{i,t+1}^D\} \end{aligned} \quad (3.5)$$

The vector of decision thresholds $\boldsymbol{\eta}_{t+1}$ minimizing $-\text{Tr}\{\mathbf{J}_{t+1}\}$ can be easily obtained by using line-search. Since the total FIM is the sum of each sensors individual FIM, the line-search minimizing $-\text{Tr}\{\mathbf{J}_{t+1}\}$ becomes decoupled at each sensor.

3.2.2. Objective Function 2: Sum of Sensor Transmission Probabilities

In this part, we assumed an ON-OFF strategy, that is, if $D_{i,t} = 1$, the sensor reports to the fusion center, otherwise it stays silent. Then, energy conservation of sensor is realized by forcing the ON probability (sensor transmission probability) $p(D_{i,t+1} = 1)$ to zero. Then, the second objective function, $f_2(\boldsymbol{\eta}_{t+1})$, the sum of sensor transmission probabilities reduces the

¹Let J be a $n \times n$ real symmetric FIM whose diagonal entries are equal to its eigenvalues $(\lambda_1, \dots, \lambda_n)$ where $\text{Tr}\{J\} = \sum_{j=1}^n \lambda_j$. Maximization of $\text{Tr}\{J\}$ does not guarantee the minimization of $\text{Tr}\{J^{-1}\} = \sum_{j=1}^n \lambda_j^{-1}$ or maximization of $\det\{J\} = \prod_{j=1}^n \lambda_j$.

number of sensors transmitting to the fusion center as,

$$\min_{\boldsymbol{\eta}_{t+1}} f_2(\boldsymbol{\eta}_{t+1}) = \sum_{i=1}^N p(D_{i,t+1} = 1) \quad (3.6)$$

where $p(D_{i,t+1} = 1) = p(z_{i,t+1} > \eta_{i,t+1})$ and

$$\begin{aligned} & \sum_{i=1}^N p(z_{i,t+1} > \eta_{i,t+1}) \\ &= \int \left\{ \sum_{i=1}^N p(z_{i,t+1} > \eta_{i,t+1} | \mathbf{x}_{t+1}) \right\} p(\mathbf{x}_{t+1} | \mathbf{D}_{1:t}) d\mathbf{x}_{t+1} \\ &\approx \frac{1}{N_S} \sum_{s=1}^{N_S} \left\{ \sum_{i=1}^N p(z_{i,t+1} > \eta_{i,t+1} | \mathbf{x}_{t+1}^s) \right\} \end{aligned} \quad (3.7)$$

The vector of decision thresholds $\boldsymbol{\eta}_{t+1}$ minimizing $f_2(\boldsymbol{\eta}_{t+1})$ as $\sum_{i=1}^N p(z_{i,t+1} > \eta_{i,t+1}) \approx 0$ can be easily obtained by setting $\boldsymbol{\eta}_{t+1} = \boldsymbol{\eta}_{UB}$ where $\boldsymbol{\eta}_{UB}$ is the vector of upper bounds on the decision thresholds.

For the Multiobjective optimization problem considered in this part, we set $\chi = \boldsymbol{\eta}_{t+1}$. We have selected the resolution of the NBI as 10. That is we have obtained 9 Pareto-optimal solutions between the two conflicting objectives. Each NBI subproblem given in Eqn. 2.28 is solved by using Matlab's "fmincon" optimization routine. For an arbitrary target trajectory, Figure 3.1 shows the Pareto-optimal front between $f_1(\boldsymbol{\eta}_{t+1})$ and $f_2(\boldsymbol{\eta}_{t+1})$ at time $t = 1$. Since we do not know the actual Pareto-front, we also obtained the Pareto-Optimal front using a multiobjective evolutionary algorithm called Non-dominated Sorting Genetic Algorithm - II (NSGA-II) as well [43]. Simulation results in Matlab, show that both algorithms yield the similar Pareto-optimal front. Note that the performance of NSGA-II heavily depends on the population size, crossover and mutation probabilities. On a 3.6 GHz computer with 8 GB RAM, for NBI and NSGA-II, the entire Pareto-optimal front shown in Figure 3.1 are obtained in 17 and 214 seconds, respectively. Note that for real-time implementation, evaluation of the Pareto-optimal front should be less than the sampling interval Δ . The processing time for the

optimization of Eqn. 2.28 can be significantly reduced using advanced solvers.

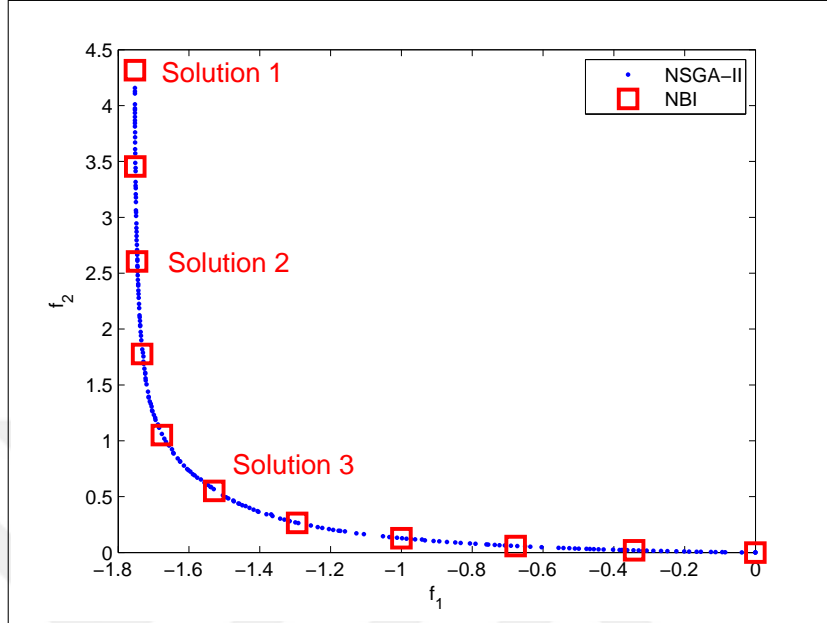


Figure 3.1. Pareto optimal front obtained with NBI and NSGA-II at time step $t = 1$. For NSGA-II we used population size 200, crossover parameter 5, mutation parameter 5, and the Pareto-optimal front is shown after 100 generations.

Having obtained the Pareto-optimal front between $f_1(\boldsymbol{\eta}_{t+1})$ and $f_2(\boldsymbol{\eta}_{t+1})$, we should decide on a solution on the Pareto optimal front. We call the solution which maximizes the trace of FIM as Solution 1. We call the solution which achieves at least 99% of the maximum trace of the FIM as Solution 2, and finally we call the solution which has the nearest Euclidean distance to the shadow minimum of the problem as Solution 3. Solution 3 has been shown as a useful trade-off solution for the multiobjective optimization problem given in [48].

3.3. NUMERICAL RESULTS

We consider $N = 9$ sensors, which are uniformly deployed in an area of size $20m \times 20m$. The target has power $P_0 = 1000$. We select the process noise parameter as $\rho = 2.5 \times 10^{-3}$. The target is sampled at every $\Delta = 0.5$ seconds. The measurement noise variance is selected as $\sigma^2 = 1$. The minimum and the maximum values of the sensor decision threshold are selected as 0 and 20 respectively. In our simulations, we track the target for 20 time steps (10 seconds)

in $T_{trials} = 200$ different trials (target trajectories).

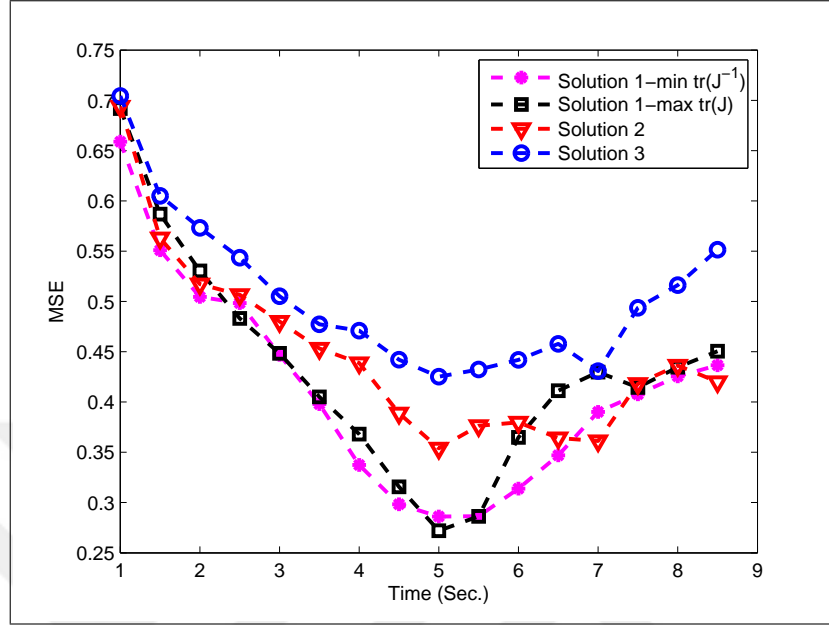


Figure 3.2. MSE at each time step of tracking

Figure 3.2 shows the sum of mean squared error on X and Y axes at each time step of tracking. In Figure 3.2, we obtain Solution 1 by both minimizing $\text{Tr}\{\mathbf{J}_{t+1}^{-1}\}$ and maximizing $\text{Tr}\{\mathbf{J}_{t+1}\}$. In terms of MSE, simulation results show that maximizing $\text{Tr}\{\mathbf{J}_{t+1}\}$ causes little suboptimality instead of minimizing $\text{Tr}\{\mathbf{J}_{t+1}^{-1}\}$. Figure 3.2 also shows that the MSE of target tracking obtained by using Solution 1 and Solution 2 are similar since they both achieve similar Fisher Information as shown in Figure 3.1. The Fisher Information of Solution 3 is relatively less than those of Solution 1 and Solution 2, so the MSE of Solution 3 is worse than MSEs of Solution 1 and Solution 2.

Figure 3.3 shows the average Number of sensors transmitting to the fusion center at each time step of tracking. Simulation results in Figure 3.3 show that while using Solution 1, during the entire observation period on the average around 4.5 sensors (half of the sensors) are transmitting at each step of tracking. On the other hand when we use Solution 2, the number of sensors transmitting to the fusion center becomes a function of the target location as well. Note that at around time step $t = 8$ (4^{th} second), the target is close to sensor 5 located at the origin, so very few sensors are reporting to the fusion center due to reduced

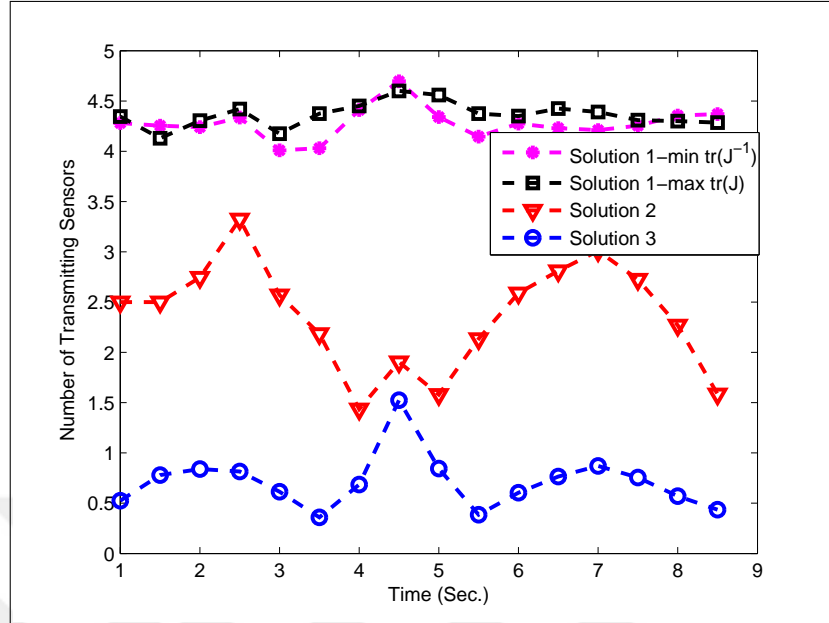


Figure 3.3. Average number of sensors transmitting to the Fusion Center at each time step of tracking

uncertainty. Around time step $t = 14$ (7^{th} second), the target is in between sensors 5, 6, 8, and 9. Due to the increased uncertainty, on the average 3 sensors report to the fusion center. Finally, when the target approaches sensor 9, sensor 9 becomes informative, the uncertainty on target location decreases, and the average number of sensors transmitting to the fusion center also decreases. Using Solution 3, only few sensors transmit to the fusion center during the entire time steps of tracking. Hence, Solution 2 becomes a good trade-off solution jointly minimizing the estimation error and the total number of transmitting sensors.

Finally, Figure 3.4 shows illustrative sensor locations and the target trajectory sampled up to time step $t = 8$. Figure 3.4 (a) shows the values of sensor decision thresholds at $t = 8$ when Solution 1 is selected from the Pareto-optimal front and Figure 3.4-(b) shows the values of sensor decision thresholds at $t = 8$ when Solution 2 is selected from the Pareto-optimal front. As can be seen from the figures, the sensor near the actual target location is assigned a relatively higher threshold value as discussed in [12]. On the other hand, if we use Solution 1, the sensors which are relatively far away from the target are assigned a small decision threshold. Since such sensors may carry negligible information about the target location,

Solution 2 increases the decision thresholds of these sensors and they are forced to stay silent.

3.4. DISCUSSIONS

In this part, we solve the adaptive binary quantization design problem for local sensors by using a MOP. The trade-off solutions between maximum Fisher Information solution and minimum sums of transmission probabilities are obtained by using computationally efficient NBI method. By using MOP, we can obtain solutions which increase the thresholds of the sensors that are far away from the target. Increasing the thresholds of such sensors has small effect on estimation but significantly reduces the average number of sensors transmitting to the fusion center at each time step of tracking.

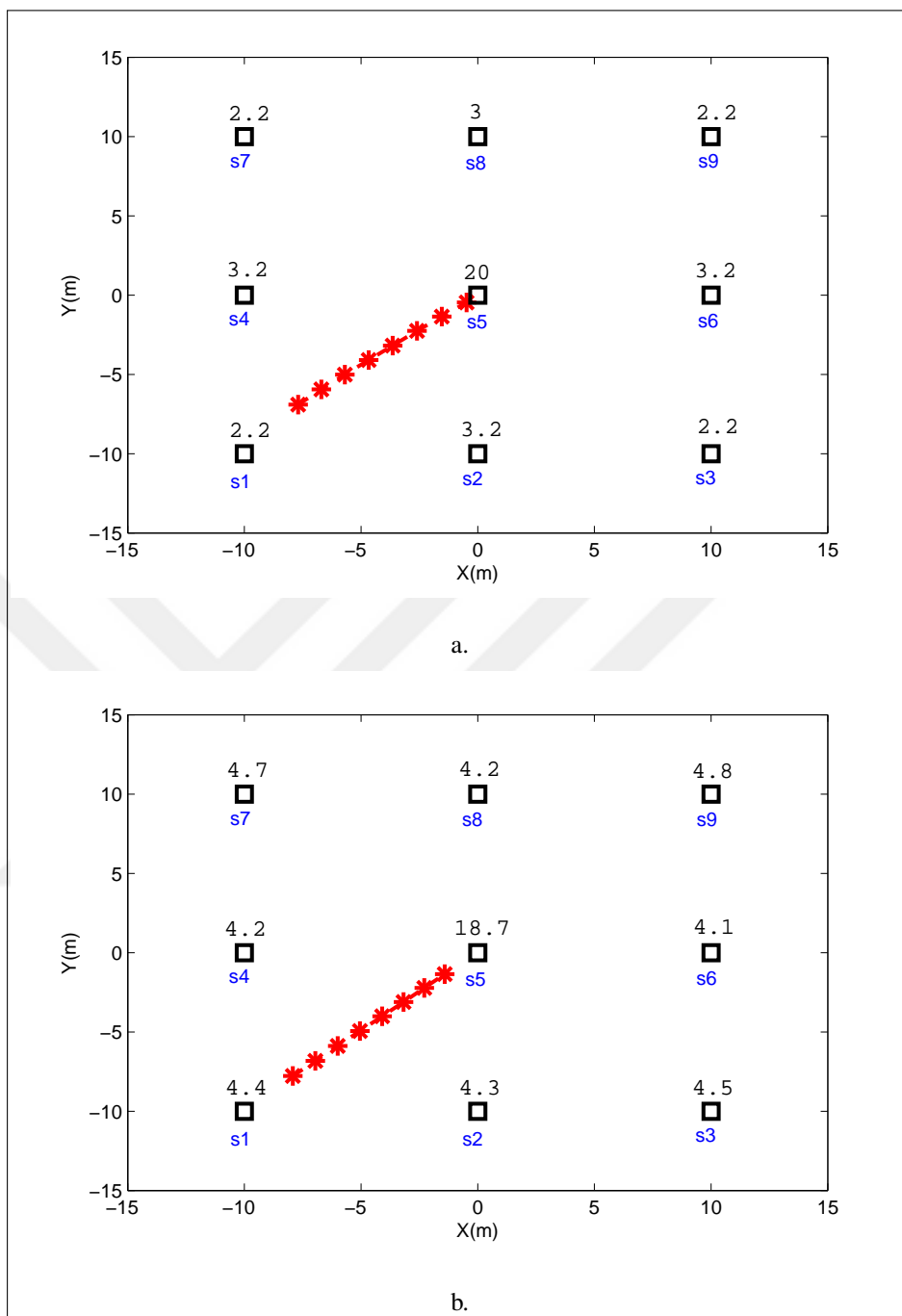


Figure 3.4. Sensor Decision Thresholds at the $t = 8^{th}$ time step of tracking (a) Solution 1, (b) Solution 2

4. ENERGY AWARE DATA TRANSMISSION OF SENSOR DECISIONS

Since a WSN is composed of energy limited sensor nodes, excessive energy consumption needs to be mitigated in order to enhance the durability of network. In [27], it is stated that as the number of hops between sensor and destination node increases more energy consumption occurs in WSN as compared to single-hop while considering energy dissipations in hardware. Moreover, in [25], the proposed clustering work for energy efficient wireless micro-sensor networks show that solely single-hop or multi-hop transmissions are not energy efficient for energy constrained nodes. In direct transmission (single-hop), sensors need high transmit power to transmit their measurements to the destination node due to long distances. Thus, this leads to quick run out of sensors batteries. In multi-hop transmission, sensor measurements need to be transmitted over multiple relays to reach FC. Considering transmitting and receiving circuit electronic energy consumption, the sensors which are closer to FC die out quickly due to huge amount of data arrive from dependent sensor nodes. Thus, clustering based 2-hop data transmission become more preferable for energy efficiency. In clustering method, there is a cluster head for each group of sensors. Sensors in each group send their measurements to the corresponding cluster head for transmission to the FC. Nevertheless, transmitting to destination node via cluster head may not be the best energy efficient way in every case due to extra energy burden on CHs. In this chapter, thus, we prefer a minimum transmission energy path (MTEP) for target tracking between sensors and FC to get rid of the drawbacks of single-hop and 2-hop transmission. In this chapter, we consider an illustrative of WSN to determine drawbacks and benefits of single-hop and cluster based 2-hop transmission. In addition, MTEP based transmission with MOP which has been proposed in previous chapter is considered to reduce further the overall energy consumption of the network by preventing redundant energy consumption in CHs.

4.1. SELECTION OF DATA TRANSMISSION PATH

There are two scenarios that sensor can forward their measurements to the destination node. One way is to direct communication with fusion center without any intermediate relays. Other path is to transmit information over one relay (2-hop) or through multiple intermediates nodes(multi-hop) to reach fusion center. In both cases, single-hop and 2-hop, energy consumption in each path need to be calculated to decide which path consumes less energy. In this chapter, we only consider 2-hop and single-hop data transmissions.

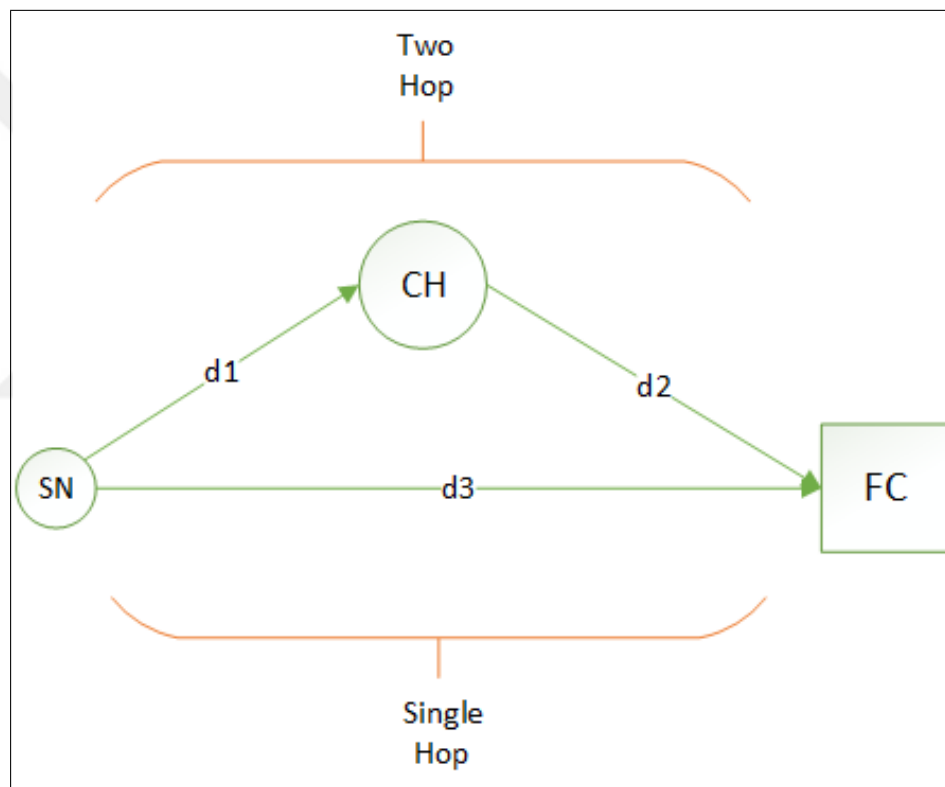


Figure 4.1. Transmission path in 2-hop and Single-hop

4.1.1. Data Transmission under Single-hop Links

In Figure 4.1, a sensor node either transmits its data to its cluster head for forwarding to the fusion center (FC) or send directly to FC. There are two cases we can consider in order to make a comparison between single-hop and 2-hop. We need to calculate energy consumption under single-hop when energy dissipations in hardware of a node during transmission as

shown in Figure 4.2.

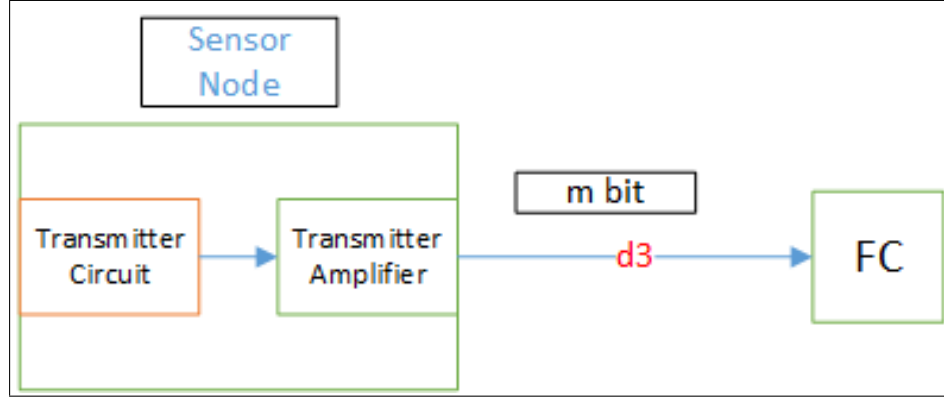


Figure 4.2. Energy consumption steps during single-hop transmission

Thus, required energy for transmitting $m - bit$ from a sensor node to FC can be expressed as,

$$E_T(m, d_{s,FC}) = E_{Tcircuit} \times m + \epsilon_{amp} \times m \times d_3^2 \quad (4.1)$$

4.1.2. Data Transmission under 2-hop Links

As regards 2-hop transmission, a sensor observation is transmitted to FC through an intermediate node as shown in Figure 4.1. Figure 4.3 show energy dissipation steps for transmission $m - bit$ observation of a sensor node to FC through a cluster head. Thus, energy required for transmitting $m - bit$ can be expressed as,

$$E_T(m, d_{i,j}) = E_{Tcircuit} \times m + \epsilon_{amp} \times m \times d_{i,j}^2 \quad (4.2)$$

where $d_{i,j}$ is the distance between transmitter sensor node and receiver sensor node. Energy required for m bit data to be received accurately at sensor j^{th} node is given by

$$E_{R,j}(m) = E_{Rcircuit} \times m \quad (4.3)$$

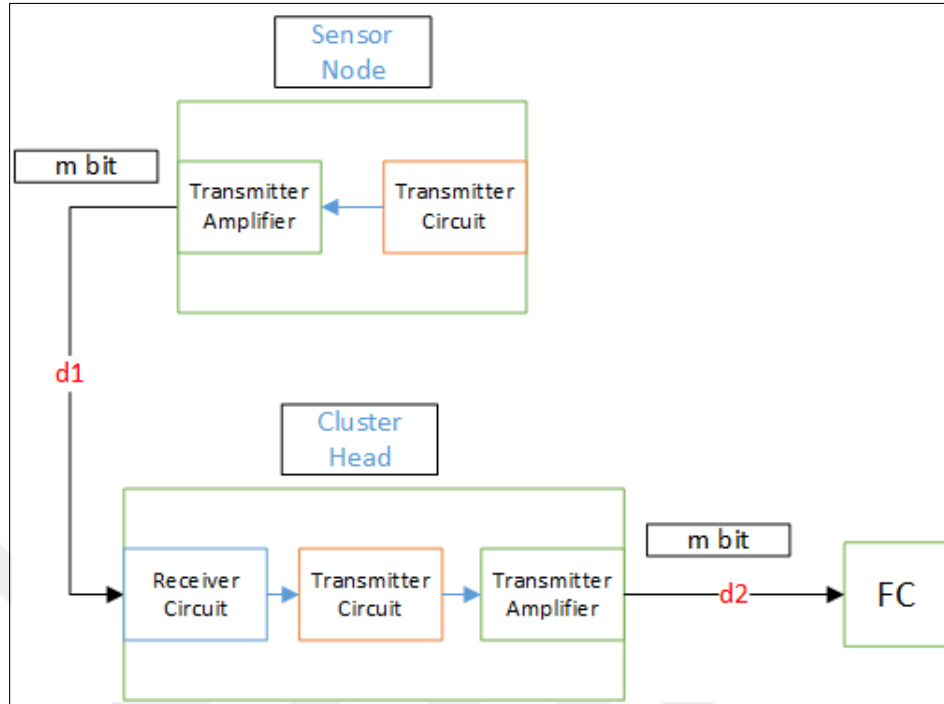


Figure 4.3. Energy consumption steps during 2-hop transmission

Required energy for transmitting m – bit to FC through a relay node as shown in Figure 4.1 would be depend on both Eqn. 4.2 and Eqn. 4.3. Therefore, energy dissipation under 2-hop transmission is expressed as,

$$\begin{aligned}
 E_T(m, d_{s,FC}) &= \{E_T(m, d_{s,CH}) + E_{R,j}(m) + E_T(m, d_{CH,FC})\} \\
 &= m \times (3 \times E_{circuit} + \epsilon_{amp} \times (d_1^2 + d_2^2)) \quad (4.4)
 \end{aligned}$$

Taking into consideration of circuit energy, 2-hop transmission can become more efficient only if Eqn. 4.1 is greater than Eqn. 4.4. Thus, this inequality can be concluded according to distance shown in Figure 4.1 as,

$$(d_3^2 - (d_1^2 + d_2^2)) > \frac{2 \times E_{circuit}}{\epsilon_{amp}} \quad (4.5)$$

According to that, 2-hop transmission requires less energy only if distance from a sensor node to FC suppresses total circuit energy consumption.

4.1.3. MTEP based Data Transmission

In previous part, we show that required energy for transmitting sensor observations basically depend on which parameters in both single-hop and 2-hop links and under which conditions they can become more energy efficient for overall network. Here, we consider MTEP in which sensor data requires less energy than using solely single-hop or 2-hop transmission.

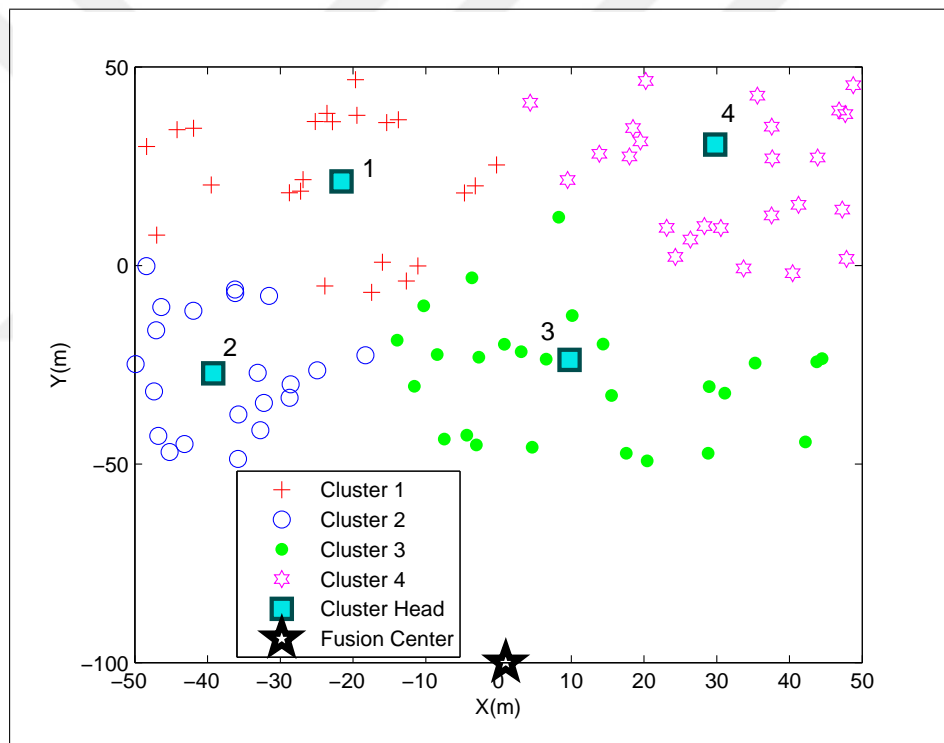


Figure 4.4. A WSN example with 4 clusters (N=100 randomly deployed sensors)

Figure 4.4 shows the considered network which has 100 sensors deployed randomly in an area with a size of 100×100 . Sensors are divided into 4 clusters where one fixed sensor are selected as cluster head. Fusion center (FC) is located out of this area with a 50 m away from nearest sensor node. We find CH nodes by using K-means clustering algorithm. K-means clustering firstly find centroids of K clusters and then groups the sensors according to minimum distance to the centroids [49]. Since there may not be a sensor node at centroid

location, we select nearest sensor node to its centroid as CH. The considered system make a comparison as given in Eqn. 4.5 between direct (single-hop) and 2-hop transmission in terms of required energy for each sensors data to reach to FC. Based on required energy, each sensor observation is transmitted to over minimum energy path. The aim is to minimize overall energy consumption of network by preventing unnecessary data load on cluster heads that leads more circuit energy consumption as well as overload communication traffics. By this way, sensors closest to fusion center more than cluster heads would sooner transmitting their observations to the destination node over single-hop links. On the other hand, sensors that would more exposure path loss in case of direct transmission to destination node prioritize 2-hop transmission with theirs corresponding cluster heads.

4.1.4. Numerical Results

In this simulation, we do not consider target tracking and we only assume each sensor send its local decision in every second of 20 seconds to the FC. Figure 4.4 shows network topology of sensors deployments in each cluster. In this part, we also assume that sensor nodes become cluster head in order according to minimum distance to central node. By this way we aim to reduce energy burden on fixed CHs. T.

Algorithm 4.1. MTEP based data transmission

```

Let  $t = 1$ 
while  $t \leq T$  do
    Calculate required energy for each sensors' data to reach FC under single-hop and
    2-hop transmission
    if  $E_{2-hop} < E_{shop}$  then
        Select 2-hop transmission
    else
        Decide Single-hop transmission
    end if
end while

```

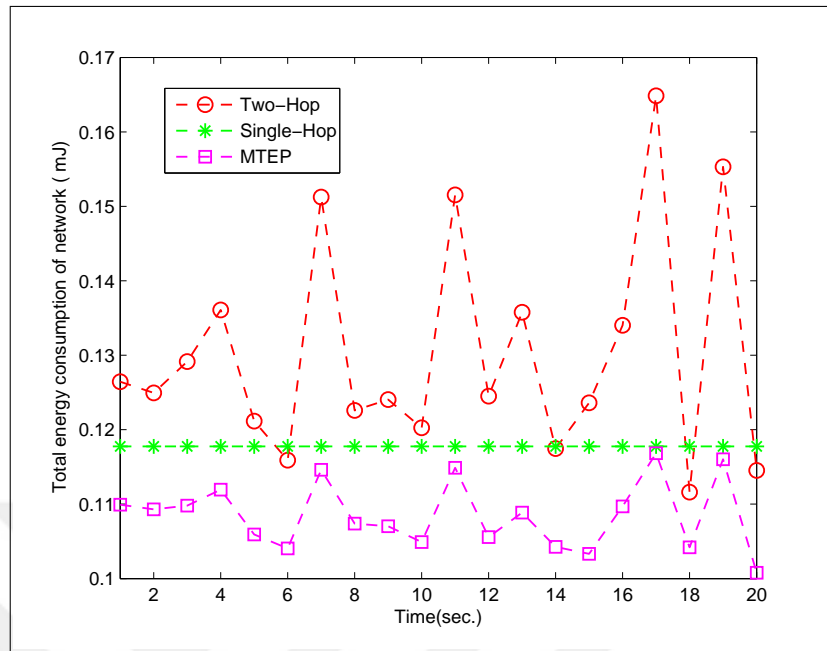


Figure 4.5. Total energy consumption of network at each second with varying CHs

Figure 4.5 shows total energy consumptions of network which are estimated in case of single-hop, 2-hop and MTEP transmissions in every second. As seen in Figure 4.5, energy requirement under single-hop remain constant due to that sensors transmit with fixed distances to FC each time step of tracking. Total energy consumption of network under 2-hop transmission varies because CH nodes changes in every second. On the other hand, the MTEP that follow minimum required energy path to reach FC consumes less energy than both solely single-hop and 2-hop transmissions at each second. This is because, MTEP based transmission compares required energy using single-hop and 2-hop for transmitting each observation of a sensor to FC as expressed Algorithm 4.1. Thus, each sensor decision follow either single-hop or 2-hop path based on total energy consumption until data reach destination node.

Nevertheless, in Figure 4.6, energy consumption of each sensor are presented under single-hop, 2-hop transmission and MTEP with fixed CH. It can be seen that majority of sensors except CH nodes use less energy in 2-hop and MTEP than single-hop transmission. In single-hop transmission, each sensor communicates with FC directly which leads high energy

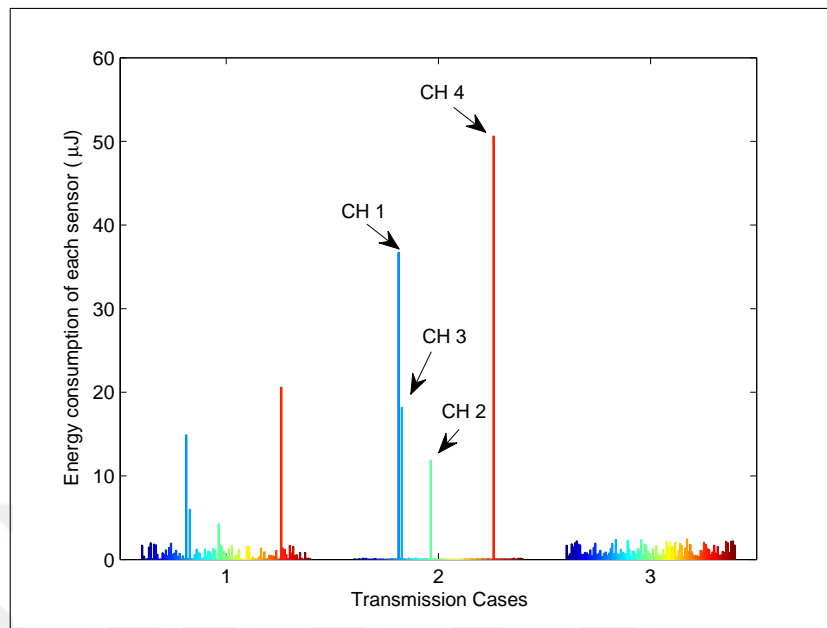


Figure 4.6. Energy consumption of each sensor in both three cases with fixed CHs (1: MTEP, 2: 2-hop, 3: Single-hop)

consumption in sensor nodes as much clearly seen in Figure 4.7.

However, in 2-hop transmission, sensors send their observations to their corresponded CH that results in less energy consumption in these sensor nodes than directly transmitting to FC. Nevertheless, under 2-hop transmission as shown in Figure 4.8, too much energy consumption occurs in CH nodes due to receiving and transmitting energy consumption for data coming from sensor nodes in cluster. Especially CHs which are away from the FC consume more energy to transmit measurements of sensor nodes in clusters.

On the other hand, massive energy consumption in CH nodes under 2-hop are halved as seen clearly in Figure 4.9 with MTEP transmission while maintaining less energy dissipation in other sensors as compared to single-hop.

Although MTEP transmission reduce the overall energy consumption of network as compared to single-hop and 2-hop, energy consumption in CHs is still high despite much less burden on CHs than 2-hop transmission. Thus, in next section we consider energy consumption under

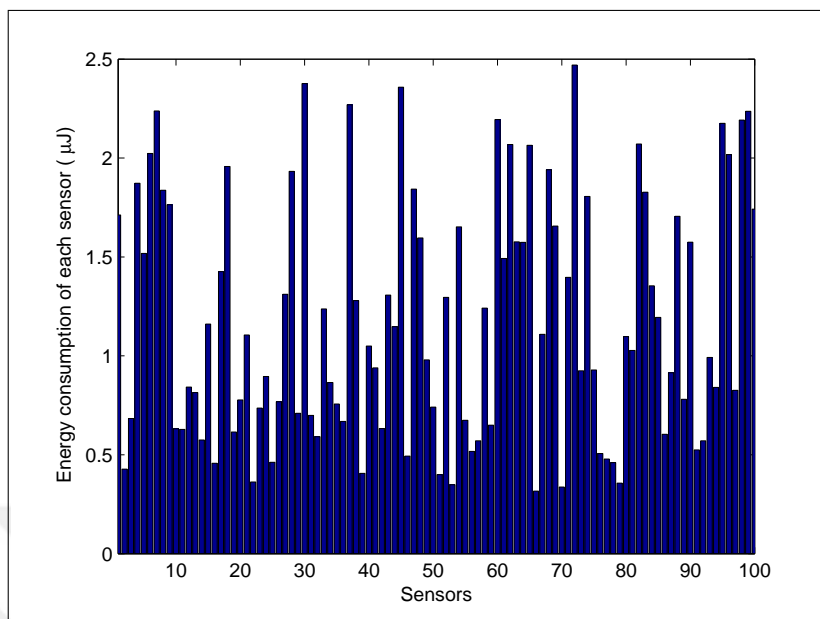


Figure 4.7. Energy consumption of each sensor under Single-hop transmission

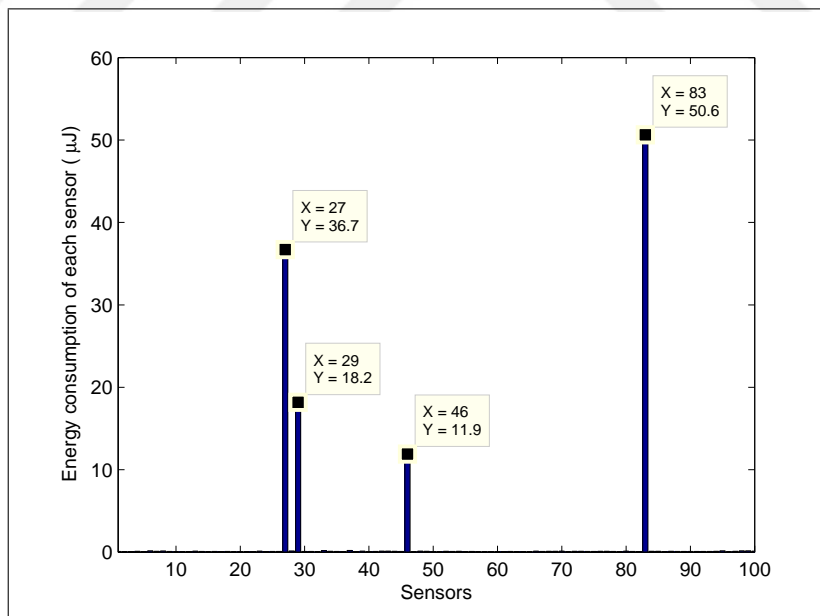


Figure 4.8. Energy consumption of each sensor under 2-hop transmission with fixed CHs

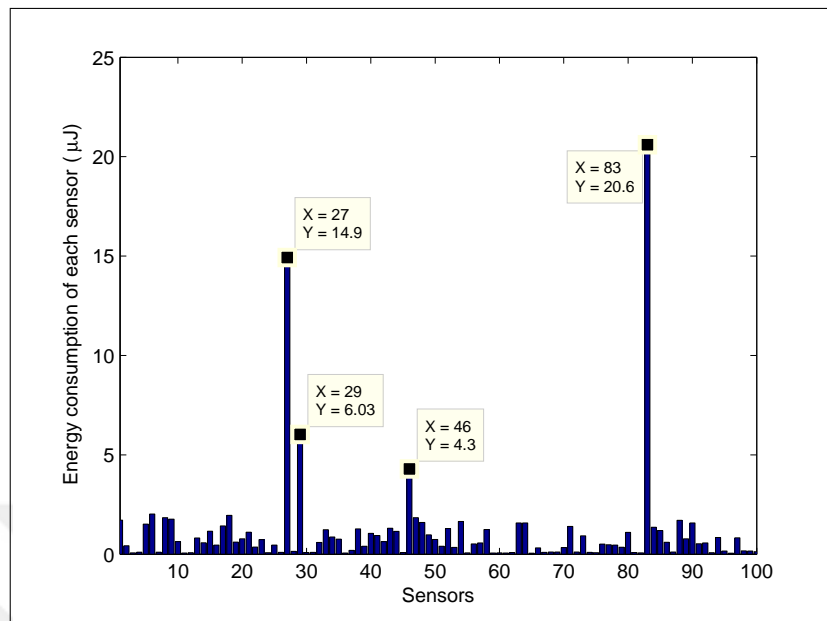


Figure 4.9. Energy consumption of each sensor under MTEP for fixed CHs

single-hop and MTEP on a sample of WSN by applying MOP method as applied in Chapter 3.

4.2. SENSOR DECISIONS WITH MOP UNDER MTEP

In the previous section, we determine under which cases data transmission in 2-hop or single-hop can be favourable based on energy requirements. In this section, we apply MOP method to minimize energy consumption by forcing less informative sensors silent under single-hop and MTEP transmission. Thus, less energy consumption occurs in both sensor nodes and CHs by preventing unnecessary transmissions. Our aim is to reduce overall network energy consumption while maintaining high estimation performance.

4.2.1. Objective Functions

Here, we consider two objective functions under MTEP transmission. Although the first objective function is same as in Section 3.2.1, we differently consider energy consumption of sensor nodes as second objective.

4.2.1.1. Objective Function 1: Trace of FIM

In this part, we use same objective function as defined in Section 3.2.1.

4.2.1.2. Objective Function 2: Total energy consumption in WSN

By considering energy consumption transmission and receiving of any m-bit sensor measurement in Eqn. 4.2 and Eqn. 4.3, Eqn. 3.6 turns into

$$\min_{\boldsymbol{\eta}_{t+1}} f_2(\boldsymbol{\eta}_{t+1}) = \sum_{i=1}^N E_{i,FC} \times p(D_{i,t+1} = 1) \quad (4.6)$$

where $E_{i,FC}$ is the required energy for transmitting from i^{th} sensor node to FC under single-hop or 2-hop.

In this study, transmitter and receiver circuit energy are taken as $E_{Rcircuit} = E_{Tcircuit} = E_{circuit} = 50nJ$ and $\epsilon_{amp} = 0.1nJ$ [25]. Let $m = 1$ in Eqn. 4.2 and Eqn. 4.3 due to that we assume binary quantization in this work.

4.2.1.3. Energy Consumption under MTEP with MOP

In Figure 4.10, $N=25$ sensors are deployed regularly in an area of 100×100 and the center node are assumed as FC. Each sensor sends its binary decisions to the nearest CH node for transmission to the FC. In this deployment, each sensor observation is transmitted to FC according to the MTEP. Under such sensor and FC deployments, MTEP every time select 2-hop due to that CHs are closest to FC than the other sensors, so none of them use single-hop due to much energy consumption.

In Figure 4.10 the sensors are divided into three groups as; primary (pink), secondary (red) and central (green). Secondary sensor nodes are also called as CH. 2-hop transmissions are in the flow direction to FC. Primary sensors send their quantized measurements taken from target to the corresponded cluster head nodes which are responsible for both transmitting

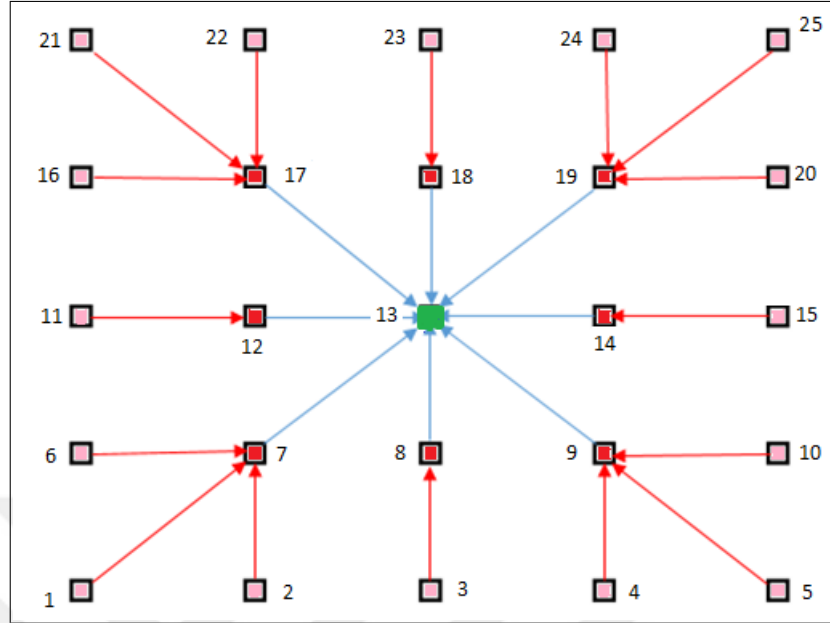


Figure 4.10. MTEP transmission tree (Red arrows:1st hop, Blue arrows:2nd hop (N=25))

their own measurements and primary sensor measurements to the FC. Required energy for transmitting 1-bit decision of any primary sensor is expressed as,

$$E_{i,FC} = E_T(1, d_{i,v(i)}) + E_{R,v(i)}(1) + E_T(1, d_{v(i),FC}) \quad (4.7)$$

$d_{i,v(i)}$ is the distance between i^{th} sensor and its cluster head $v(i)$. $E_T(1, d_{i,v(i)})$ is the required energy for transmitting 1-bit decision of a primary sensor to its cluster head. Cluster head $v(i)$ needs $E_{R,v(i)}(1)$ energy to receive 1-bit measurement of i^{th} sensor. In addition, cluster head requires also energy $E_T(1, d_{i,v(i)})$ in order to transmit this bit to the FC with a distance $d_{v(i),FC}$. On the other side, if a i^{th} sensor is a cluster head required energy turns to

$$E_{i,FC} = E_T(1, d_{i,FC}) \quad (4.8)$$

As we assume central sensor node is also FC, required energy for transmitting data of central sensor node to FC are assumed zero.

4.2.1.4. Energy Consumption under Single-hop Links with MOP

In this part, same sensor deployments are used as shown in Figure 4.10. In contrast, all sensor send their measurement directly to the FC without any relay nodes under single-hop transmission. The required energy of each sensor to send its measurement to the FC is depend on distance between FC and sensor i . Thus, transmission energy of each sensor turns to a simple form as,

$$E_{i,FC} = E_T(1, d_{i,FC}) \quad (4.9)$$

4.2.2. Numerical Results

We consider $N = 25$ sensors, which are uniformly deployed in an area of size $100m \times 100m$ as shown in Figure 4.10. Target has a power of $P_0 = 1000$. Process noise is taken as $\rho = 2.5 \times 10^{-3}$. Target are sampled at every $\Delta = 2$ seconds. Threshold values are varying from 0 to 20. $N = 1000$ particles are used for particle filter method. Target is tracked along 40 seconds for each of its 50 different trajectories. The starting point of the target trajectory for each trial again is derived from the $p(\mathbf{x}_0)$ distribution. Let l be number of trial ($l \in 1, 2, \dots, T = 50$) and t be target steps in each trial, estimated mean square error (MSE) is calculated as,

$$MSE(t) = \frac{1}{T} \sum_{l=1}^T [(\mathbf{x}_t^l(1) - \hat{\mathbf{x}}_t^l(1))^2 + (\mathbf{x}_t^l(2) - \hat{\mathbf{x}}_t^l(2))^2] \quad (4.10)$$

where in the l^{th} trial (40 sec. target observation) \mathbf{x}_t and $\hat{\mathbf{x}}_t$ are the actual and estimated target states at sample t respectively.

For an arbitrary target trajectory, Figure 4.11 shows the Pareto-optimal fronts between $f_1(\boldsymbol{\eta}_{t+1})$ and $f_2(\boldsymbol{\eta}_{t+1})$ at time $t = 1$ obtained by NBI method under both single-hop and MTEP. As seen in Figure 4.11, instead of selecting sensor threshold values that maximizes FI under single-hop and MTEP transmission, the solution obtained by MOP reduce total energy consumption

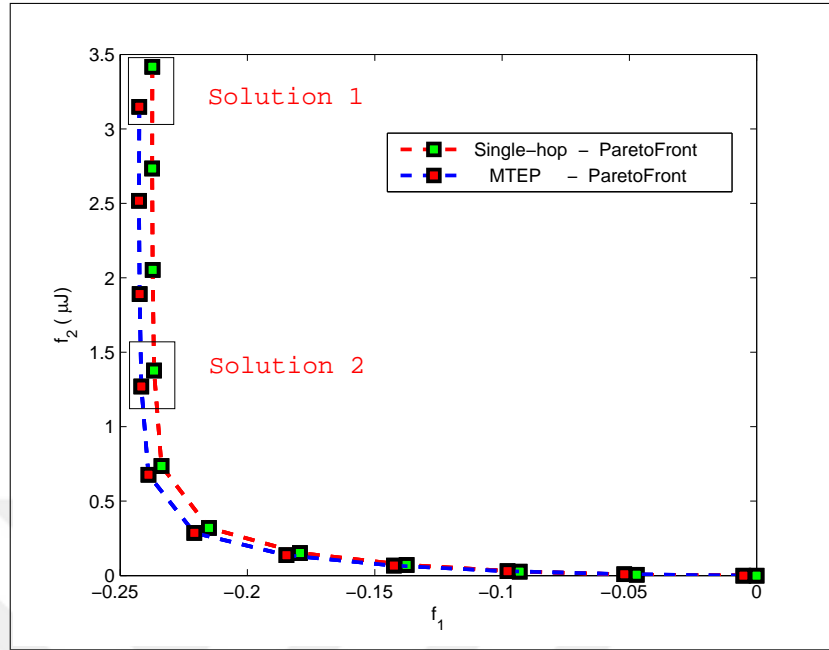


Figure 4.11. Pareto optimal front under Single-hop and 2-hop

significantly while maintaining almost same FI.

Figure 4.12 show the total mean squared error in the X and Y axes (MSE). Figure 4.12 give a comparison between sensor threshold values obtained by maximizing $\text{Tr}\{\mathbf{J}_{t+1}\}$ (Solution 1) and those obtained by MOP method (Solution 2). In addition, MTEP transmission is presented in Figure 4.12 as using Solution 2. It is clear that all three methods yield nearly similar estimation performance.

Figure 4.13 shows the average number of sensors transmitting at each time step of tracking. Simulation results presented in Figure 4.13 give information on number of sensors transmitting to FC under Solution 1 and Solution 2. Nearly half of the total number of sensors, about 12, are transmitting under single-hop transmission while maximizing $\text{Tr}\{\mathbf{J}_{t+1}^{-1}\}$ (Solution 1). However, number of transmitting sensors vary approximately between 4-7 sensors while using Solution 2 in both single-hop and MTEP transmission.

Figure 4.14 shows average total energy consumption of $T = 50$ trials for each step of

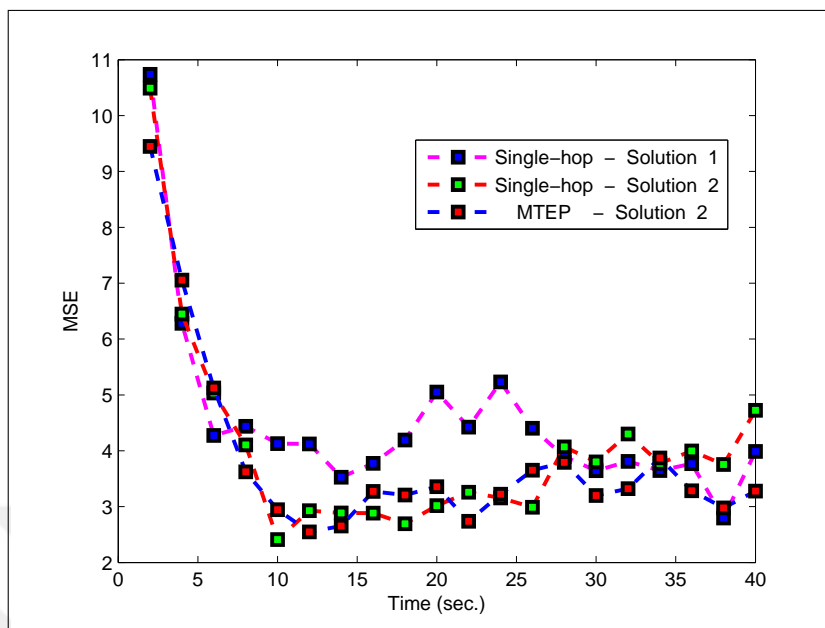


Figure 4.12. MSE at each time step of tracking

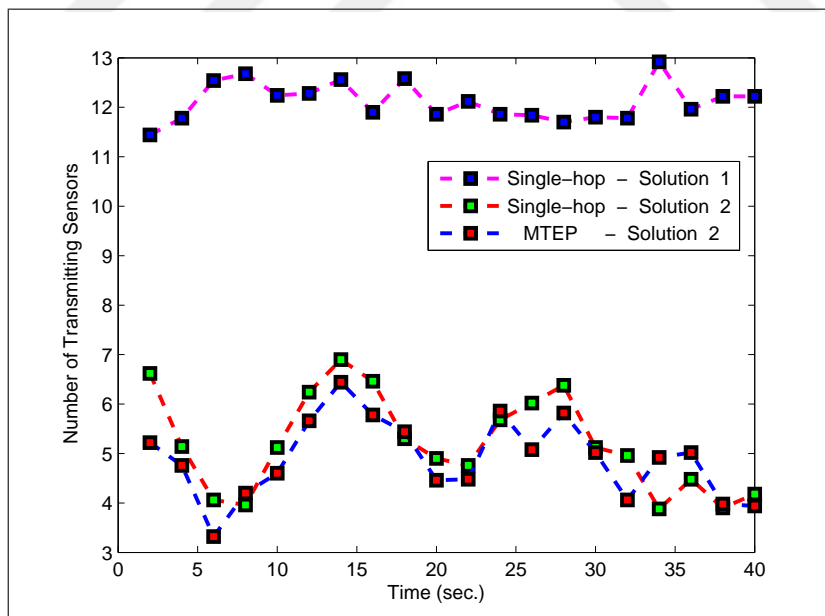


Figure 4.13. Average number of sensors transmitting to FC at each time step of tracking

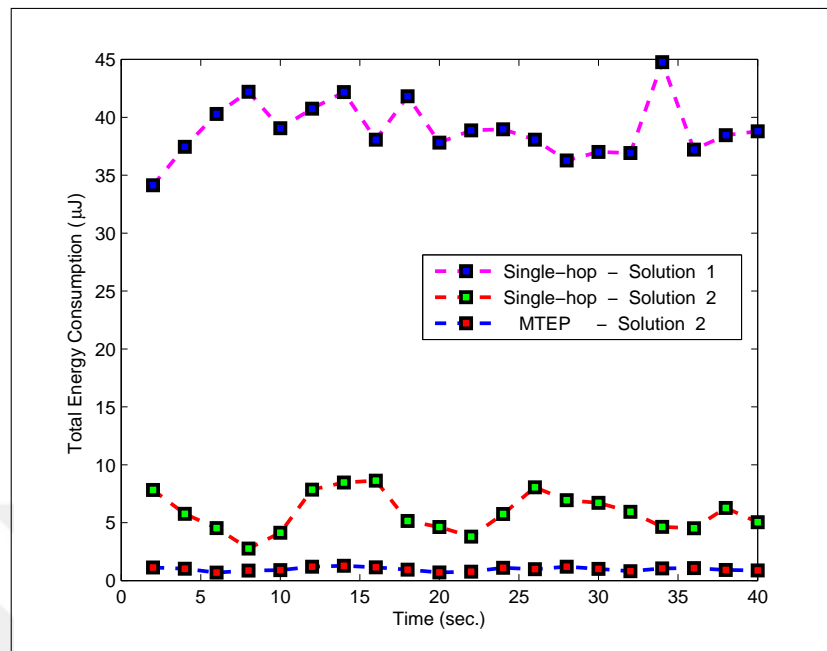


Figure 4.14. Total energy consumption in WSN

target tracking during transmission of sensors measurements in three cases mentioned above. As shown, total consumed energy of network in Solution 2 which is obtained by applying MOP becomes much less than that in Solution 1 which is obtained by maximizing $\text{Tr} \{ \mathbf{J}_{t+1} \}$. Required energy decreases dramatically, because the number of sensors is reduced by applying MOP as observed in Figure 4.13. Furthermore, consumed energy in MTEP transmission is less than single-hop transmission as shown in Figure 4.14 while both have nearly same number of sensors transmitting to FC as shown Figure 4.13(b). Required transmission energy for primary sensors to transmit their measurements to nearest sensor node(cluster head) decreases due to reduced distance under 2-hop transmission. Total energy consumption of considered WSN in Figure 4.10 under MTEP transmission is much less than that under single-hop transmission even if we consider the circuit energy consumption of cluster head nodes during receiving and transmitting.

4.3. DISCUSSIONS

In this part, a MOP is provided for minimizing energy consumption with estimation error in WSN instead of minimizing sensor probabilities. Simulation results show that, less energy is consumed for target tracking while estimation performance are similar with sensor thresholds obtained using MOP. Furthermore, proposed MTEP transmission which is more energy efficient than single-hop and 2-hop transmission enable sensors that are far away from target to transmit their measurements with less energy to FC. In addition, overload energy consumption in CHs are reduced with MOP under MTEP transmission.



5. TDMA BASED MAC SCHEME FOR TRANSMISSION OF DECISION UNDER FADING CHANNELS

In previous chapters, we consider perfect channels between sensors and the fusion center for target tracking, but we assume sensors transmit binary decisions to a distant fusion center over fading noisy channels in this chapter. Under channel fading and noise, we first determine the optimal local sensor decision thresholds by first maximizing the mutual information between received sensor measurements and the target location. We then determine the optimal sensor thresholds by minimizing the error in estimation by minimizing the trace of the C-PCRLB matrix. In our formulation, the fusion center employs hard decision decoding and arrive binary decisions for each sensor transmissions. Different from the channel fading models presented in [4, 32–34] where the transmission error occurs as a function of received signal amplitude, in our formulation transmission errors becomes a function of each sensor transmission duration. We employ a person by person optimization method, in order to determine each sensors local decision threshold. Determining the optimal sensor decision thresholds by maximizing the mutual information or by minimizing trace of C-PCRLB become computationally costly. Therefore, we also used two suboptimal metrics to determine the optimal sensor thresholds where the first one is an upperbound on mutual information (sum of individual sensor mutual information) and the second one is a lower bound on the trace of C-PCRLB (trace of Fisher Information Matrix).

5.1. MEDIUM ACCESS MODEL

In this section, we consider sensors have access to the transmission medium in a TDMA manner as shown in Fig. 5.1. In its allocated time interval, each sensor employs an ON-OFF

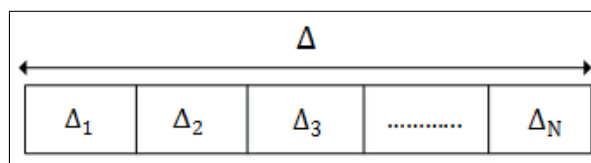


Figure 5.1. Time Division Multiple Access

strategy, and transmits the waveform $\varphi_{i,t}(n)$ according to,

$$\varphi_{i,t}(n) = \begin{cases} \sqrt{2P_T} \cos(2\pi f_0 n), & n \in \{0, 1, \dots, S_i^t - 1\} \text{ if } D_{i,t} = 1 \\ 0 & \text{if } D_{i,t} = 0 \end{cases} \quad (5.1)$$

where P_T is the transmit signal power, S_i^t is the number of samples transmitted from sensor i at time step t . Note that $f_0 = f_m/f_s$ where f_m is the carrier frequency and f_s is the sampling rate, then $0 < f_0 < 0.5$. Let $\Delta^t \triangleq [\Delta_1^t, \Delta_2^t, \dots, \Delta_N^t]$ be the time allocation vector to all sensors at time step t . For sensor i , number of samples transmitting the signal $\varphi_{i,t}(n)$ is then expressed as $S_i^t = \Delta_i^t \times f_s$ samples. Here, the total time duration for sensors to transmit their decisions to fusion center should be less than the time step of tracking, $\sum_{i=1}^N \Delta_i^t \leq \Delta$.

In this part, at each time step of tracking, we first consider equal time allocations to all sensors in the WSN to transmit their measurements to the fusion center, i.e., $\Delta_i^t = \Delta/N$ for $i \in \{1, 2, \dots, N\}$ and $t \in \{1, 2, \dots, T\}$ where we define T as the total number of time steps in tracking. Later in the chapter, we propose a proportional time sharing approach where the informative sensors about the target are given more time to transmit their decisions hence decreasing their probability of transmission errors.

5.2. WIRELESS CHANNEL EFFECTS

In this section we jointly consider path loss and narrowband multipath fading effects which distorts the transmitted sensor waveforms. Let $\tilde{\varphi}_{i,t}(n)$ represents the signal received from sensor i at the fusion center. $\tilde{\varphi}_{i,t}(n)$ then has the form,

$$\tilde{\varphi}_{i,t}(n) = \begin{cases} A \cos(2\pi f_0 n + \phi) + w(n) & \text{if } D_{i,t} = 1 \\ w(n) & \text{if } D_{i,t} = 0 \end{cases} \quad (5.2)$$

Here, $w(n)$ is the zero mean white Gaussian channel noise with variance σ_w^2 . Under narrowband fading model, the signal gain A and the phase offset ϕ are independent random variables. Phase offset ϕ is uniformly distributed between 0 and 2π . The gain A is Rayleigh

distributed with probability density function (PDF),

$$p(A) = \frac{2A}{P_R} \exp\left(-\frac{A^2}{P_R}\right) \quad (5.3)$$

P_R is the power of the received waveform which is a function of the distance between sensor and the fusion center. In this section, we consider the simplified path loss model between sensor i (transmitter) and the fusion center (receiver) as,

$$P_R = \frac{P_T}{(d_{i,FC})^2} \quad (5.4)$$

where $d_{i,FC}$ represents the distance between sensor i and the fusion center. In this part, we assume that the fusion center is located far from the sensor field. Then $d_{1,FC} \approx d_{2,FC} \approx \dots \approx d_{N,FC} \approx d_{FC}$ where d_{FC} represents the distance between sensor field and fusion center.

For the signal received from sensor i , the fusion center employs hard decision decoding to conclude the decision of sensor i . Upon employing the periodogram receiver [50], under Rayleigh fading channel, the test statistic for $\tilde{\varphi}_{i,t}(n)$, $T(\tilde{\varphi}_{i,t})$ is obtained as,

$$T(\tilde{\varphi}_{i,t}) = \frac{1}{S_i^t} \left| \sum_{n=0}^{S_i^t-1} \tilde{\varphi}_{i,t}(n) \exp(-j2\pi f_0 n) \right|^2 \quad (5.5)$$

Then, the probabilities of the received binary decision $\{0, 1\}$ for the i^{th} sensor is expressed as [50],

$$\begin{aligned} P_{1|0} &\triangleq P(R_{i,t} = 1 | D_{i,t} = 0) \\ &= P(T(\tilde{\varphi}_{i,t}) > \gamma | D_{i,t} = 0) = \exp\left(-\frac{\gamma}{\sigma_w^2}\right) \end{aligned} \quad (5.6)$$

and

$$\begin{aligned}
 P_{1|1} &\triangleq P(R_{i,t} = 1|D_{i,t} = 1) \\
 &= P(T(\tilde{\varphi}_{i,t}) > \gamma|D_{i,t} = 1) = \exp\left(-\frac{\gamma}{S_i\left(\frac{P_r}{4}\right) + \sigma_w^2}\right)
 \end{aligned} \tag{5.7}$$

where γ is the threshold used for signal reception at the fusion center.

Given target location \mathbf{x}_t , the joint PDF of received sensor decisions $\mathbf{R}_t = [R_{1,t}, \dots, R_{N,t}]$ of N sensors is described as,

$$P(\mathbf{R}_t|\mathbf{x}_t) = \prod_{i=1}^N P(R_{i,t}|\mathbf{x}_t) \tag{5.8}$$

where

$$\begin{aligned}
 P(R_{i,t} = 1|\mathbf{x}_t) &= P_{1|0}P(D_{i,t} = 0|\mathbf{x}_t) + P_{1|1}P(D_{i,t} = 1|\mathbf{x}_t) \\
 P(R_{i,t} = 0|\mathbf{x}_t) &= P_{0|0}P(D_{i,t} = 0|\mathbf{x}_t) + P_{0|1}P(D_{i,t} = 1|\mathbf{x}_t)
 \end{aligned} \tag{5.9}$$

and $P_{0|0} = 1 - P_{1|0}$, $P_{0|1} = 1 - P_{1|1}$.

5.3. FUSION OF SENSOR DECISIONS UNDER FADING CHANNELS

Based on the received sensor decisions, the MMSE estimate of the target location is obtained as,

$$\hat{\mathbf{x}}_t = \int \mathbf{x}_t p(\mathbf{x}_t|\mathbf{R}_t) d\mathbf{x}_t \tag{5.10}$$

Here $p(\mathbf{x}_t|\mathbf{R}_t)$ represents the posterior PDF of the target location upon the reception of sensor decisions at time t . As a result of Bayes rule $p(\mathbf{x}_t|\mathbf{R}_t) \propto P(\mathbf{R}_t|\mathbf{x}_t)p(\mathbf{x}_t)$. Here, $P(\mathbf{R}_t|\mathbf{x}_t)$ is computed as defined in (5.8). $p(\mathbf{x}_t) \approx p(\mathbf{x}_t|\mathbf{R}_{t-1})$ is the prior probability of target location

that is the probability distribution of \mathbf{x}_t upon the reception of sensor decisions \mathbf{R}_{t-1} . We compute (5.10) numerically using the sequential importance resampling (SIR) based Particle Filtering method as described next.

A SIR based Particle Filtering method as shown in Algorithm 3.1. Here $p(\mathbf{x}_t|\mathbf{R}_t)$ is approximated by particles \mathbf{x}_t^s and their weights w_t^s .

$$p(\mathbf{x}_t|\mathbf{R}_t) \approx \sum_{s=1}^{N_s} w_t^s \delta(\mathbf{x}_t - \mathbf{x}_t^s) \quad (5.11)$$

where N_s is the total number of particles, and $w_t^s = 1/N_s$. Then, \mathbf{x}_{t+1}^s 's are obtained by propagating \mathbf{x}_t^s using (2.1) to obtain the prior

$$p(\mathbf{x}_{t+1}|\mathbf{R}_t) \approx \frac{1}{N_s} \sum_{s=1}^{N_s} \delta(\mathbf{x}_{t+1} - \mathbf{x}_{t+1}^s) \quad (5.12)$$

During the propagation step of the algorithm, we determine the vector of sensor decision thresholds $\boldsymbol{\eta}_t$ and time allocations of each sensor Δ_i^t 's using $p(\mathbf{x}_{t+1}|\mathbf{R}_t)$. After the fusion center receives the binary sensor decisions \mathbf{R}_{t+1} over erroneous channels with decision error probabilities $P_{1|0}$ and $P_{0|1}$ from N sensors, the particle weights are updated and the target location is estimated for $t + 1$.

5.4. OPTIMIZATION OF SENSOR DECISION THRESHOLDS

At time step t of tracking, the sensor decision thresholds for the next time step of tracking $\boldsymbol{\eta}_{t+1}$ are obtained according to a Person by person optimization algorithm as follows:

Algorithm 5.1. Evaluation of the optimal sensor decision thresholds

(1) Let $c = 0$, N sensor thresholds are initialized by an arbitrary value $\boldsymbol{\eta}_{t+1}^c = [\eta_{1,t+1}^c, \eta_{2,t+1}^c \cdots \eta_{N,t+1}^c] = [1 \ 1 \ \dots \ 1]$.

(2) $i = 1$

while $i \leq N$ **do**

$\eta_{i,t+1}^{c+1} = \arg \max_{\eta \in \{\eta_{min}, \eta_{max}\}} \text{Information}(\eta_{1,t+1}^{c+1}, \eta_{2,t+1}^{c+1} \cdots \eta, \dots, \eta_{N,t+1}^c)$.

$i = i + 1$.

end while

(3) If $\boldsymbol{\eta}_{t+1}^{c+1} \approx \boldsymbol{\eta}_{t+1}^c$, Stop. Otherwise, set $c = c + 1$, and go to the Step (2).

For information maximization, either Mutual Information or Fisher Information can be used. By considering impairments of the wireless channels, entropy in Eqn. 2.13 for received sensor decisions $\mathbf{R}_t = [R_{1,t}, \dots, R_{N,t}]$ turns to,

$$\begin{aligned}
 H(\mathbf{R}_{t+1}) &= - \sum_{\mathbf{R}_{t+1}} P(\mathbf{R}_{t+1}) \log_2 P(\mathbf{R}_{t+1}) \\
 &= - \sum_{r_1=0}^1 \cdots \sum_{r_N=0}^1 P(R_{1,t+1} = r_1, \dots, R_{N,t+1} = r_N) \\
 &\quad \times \log_2 P(D_{1,t+1} = r_1, \dots, R_{N,t+1} = r_N)
 \end{aligned} \tag{5.13}$$

where

$$\begin{aligned}
 P(R_{1,t+1} = r_1, \dots, R_{N,t+1} = r_N) &\approx \sum_{s=1}^{N_s} w_{t+1}^s \\
 &\times \left[\prod_{i=1}^N \left(\sum_{d_i=0}^1 P(R_{i,t+1} = r_i | D_{i,t+1} = d_i) P(D_{i,t+1} = d_i | \mathbf{x}_{t+1}^s) \right) \right]
 \end{aligned} \tag{5.14}$$

Secondly, the conditional entropy in Eqn. 5.15 is modified as,

$$\begin{aligned}
H(\mathbf{R}_{t+1}|\mathbf{x}_{t+1}) &= - \int_{\mathbf{x}_{t+1}} \sum_{i=1}^N \sum_{r_i=0}^1 \\
&\left[\left(\sum_{d_i=0}^1 P(R_{i,t+1} = r_i | D_{i,t+1} = d_i) P(D_{i,t+1} = d_i | \mathbf{x}_{t+1}) \right) \right. \\
&\left. \log_2 \left(\sum_{d_i=0}^1 P(R_{i,t+1} = r_i | D_{i,t+1} = d_i) P(D_{i,t+1} = d_i | \mathbf{x}_{t+1}) \right) \right] \\
&\times p(\mathbf{x}_{t+1}) d\mathbf{x}_{t+1} \tag{5.15}
\end{aligned}$$

detailed derivation can be found in Equation (A.5). Note that computation of Eqn. 5.13 requires 2^N summations which may become computationally expensive when N is large. Rather than maximizing $I(\mathbf{x}_{t+1}, \mathbf{R}_{t+1})$, one can maximize its upperbound [51],

$$I(\mathbf{x}_{t+1}, \mathbf{R}_{t+1}) \leq \sum_{i=1}^N I(\mathbf{x}_{t+1}, R_{i,t+1}) \tag{5.16}$$

where $I(\mathbf{x}_{t+1}, R_{i,t+1}) = H(R_{i,t+1}) - H(R_{i,t+1}|\mathbf{x}_{t+1})$. For sensor i , $H(R_{i,t+1})$ and $H(R_{i,t+1}|\mathbf{x}_{t+1})$ can be computed similar to Eqn. 2.13 and Eqn. 5.15.

As regards FI, $\mathbf{J}_{i,t+1}^D$ in Eqn. 5.18 turns to,

$$\begin{aligned}
\mathbf{J}_{i,t+1}^D &\approx \\
&\sum_{s=1}^{N_S} \frac{1}{N_S} \left\{ \sum_{r_i=0}^1 \frac{1}{\left(\sum_{d_i=0}^1 P(R_{i,t+1} = r_i | D_{i,t+1} = d_i) P(D_{i,t+1} = d_i | \mathbf{x}_{t+1}^s) \right)} \right. \\
&\left. \left[\sum_{d_i=0}^1 P(R_{i,t+1} = r_i | D_{i,t+1} = d_i) \left(\frac{\partial}{\partial \mathbf{x}_{t+1}} P(D_{i,t+1} = d_i | \mathbf{x}_{t+1}^s) \right) \right]^2 \right\} \tag{5.17}
\end{aligned}$$

In summary, \mathbf{J}_{t+1} is written as,

$$\begin{aligned}\mathbf{J}_{t+1} &= \mathbf{J}_{t+1}^D + \mathbf{J}_{t+1}^P \\ &= \sum_{i=1}^N \mathbf{J}_{i,t+1}^D + \mathbf{J}_{t+1}^P\end{aligned}\quad (5.18)$$

detailed derivation are given in Equation (B.4). For trace of fisher information we can maximize $\mathbf{J}_{i,t+1}^D$ to find optimum threshold for each sensor, because \mathbf{J}_{t+1}^P is constant. Thus, maximizing trace of $\mathbf{J}_{i,t+1}^D$ is same as to maximize trace of total fisher information \mathbf{J}_{t+1} . In contrast, we can only minimize trace of inverse total fisher information \mathbf{J}_{t+1} to obtain optimum threshold for each sensor. Therefore, trace of inverse of total fisher information takes more time find optimum thresholds than trace of total fisher information as shown in Table 5.2.

Since the computation of exact mutual information $I(\mathbf{x}_{t+1}, \mathbf{R}_{t+1})$ is computationally costly, we also maximize mutual information, by maximizing its upperbound presented in Eqn. 5.16. We maximize the Fisher Information by minimizing the trace of the inverse Fisher Information matrix. We then maximize Fisher Information by maximizing the trace of the Fisher Information matrix which is a computationally less demanding metric.

At step 2 of Algorithm 5.1, the search interval of η is determined by the minimum and the maximum distances between target and sensor location. Since the minimum distance between sensor and target location $d_{min} = 0$, $\eta_{max} = \sqrt{P_0}$. Similarly, since the maximum distance between sensor and target location is d_{max} meters, $\eta_{min} = \sqrt{\frac{P_0}{1+d_{max}^2}}$. In order to get the search space between η_{min} and η_{max} , d is increased with steps of 1 meters between d_{min} and d_{max} .

5.5. NUMERICAL RESULTS

In this section, we compare the MSE performances of four different metrics, namely (exact) mutual information, upperbound on mutual information, trace of inverse Fisher Information

matrix, and trace of Fisher Information matrix. Considered simulation parameters are summarized in Table 5.1.

Table 5.1. Simulation parameters

Parameters	Values
Number of Sensors	9
Area	30m×30m
Fusion center location	(100,0)
Source Power (P_0)	1e4 W
R_b	10 bit/sec
Transmit Power (P_T)	10 W
Channel Noise (σ_w^2)	1
Measurement Noise (σ_n^2)	1
$P_{1 0}$	0.01
Number of Trials	100

In Fig 5.2, we present the target tracking performance of the local sensor decision rules when the channels between sensors and the fusion center are ideal. The simulation results show that all four metrics yield similar estimation performance. Nevertheless, exact mutual information takes long time to obtain sensor decision thresholds at each time step of tracking as compared to other metrics as shown in Table 5.2 due to 2^N summations in Eqn. 2.13.

Table 5.2. Execution time to obtain optimum sensor thresholds comparison

Information Metrics	Elapsed Time (sec.)
Exact MI	190
Upperbound MI	0.3
Trace of Inverse FI	3.7
Trace of FI	0.4

Fig 5.3 shows the target tracking performance under fading channels. The simulation results show that binary quantization thresholds obtained by maximizing the mutual information

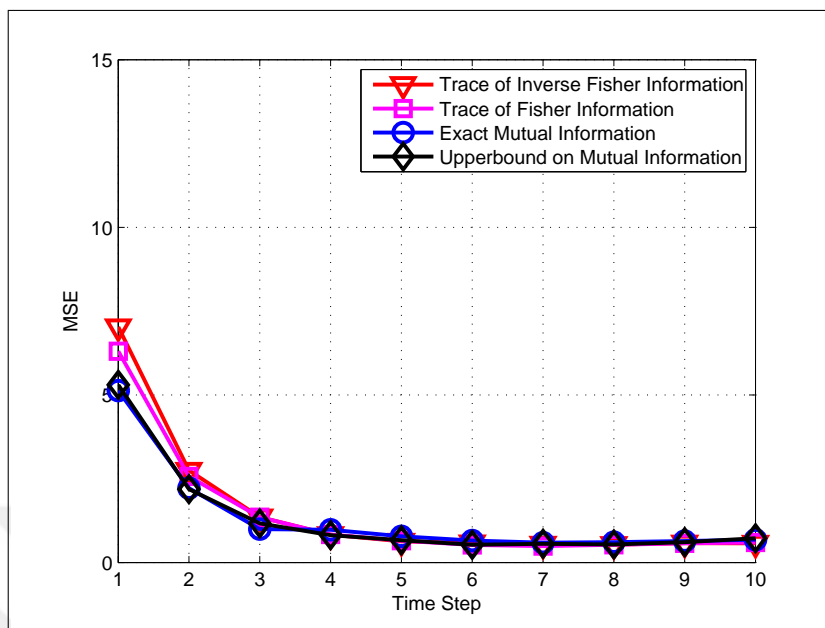


Figure 5.2. Target tracking performance of information metrics under ideal channels, $N = 9$

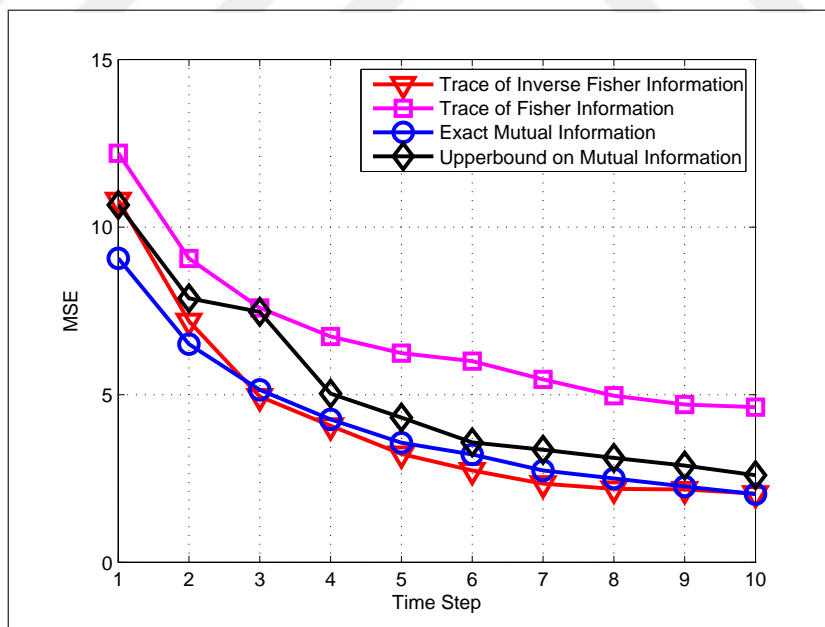


Figure 5.3. Target tracking performance of information metrics fading channels, $N = 9$.

and minimizing the trace of inverse FIM yield similar estimation performance. Among the suboptimal metrics the upperbound of the mutual information yield better estimation performance than that of trace of FIM.

5.6. PROPORTIONAL TIME ALLOCATION

In the previous section, we analyze the performance of different binary quantizer metrics under fading channels. We assume that the total available time is equally distributed among sensors. In this scenario, all sensors are treated equally. On the other hand, depending on the target location, some sensor transmissions may become more informative and if such sensors are allocated more time, their transmissions are less subject to channel errors. In this section, we study proportional time allocation (PTA) methods, so that the informative sensors are allocated more time and sensors far away from the target location are allocated less time and even they are forced to stay silent.

In this section, we consider the upperbound on Mutual Information as the performance metric, since its easy to compute and yield better estimation performance than that of trace of FIM.

5.6.1. PTA maximizing the upperbound on Mutual Information

In this PTA scheme, at each time step of tracking, the total available time Δ is distributed among sensors in order to maximize the upperbound on the mutual information, i.e.,

$$\begin{aligned} & \max_{\Delta_1, \dots, \Delta_N} \sum_{i=1}^N I(\mathbf{x}_{t+1}, R_{i,t+1}) \\ \text{such that} \quad & \sum_{i=1}^N \Delta_i \leq \Delta \end{aligned} \tag{5.19}$$

5.6.2. PTA with respect to individual Mutual Information

In this PTA scheme, at each time step of tracking, the total available time Δ is distributed among sensors relatively to their individual mutual information,

$$\Delta_i = \Delta \times \frac{I(\mathbf{x}_{t+1}, R_{i,t+1})}{\sum_{i=1}^N I(\mathbf{x}_{t+1}, R_{i,t+1})} \quad (5.20)$$

5.6.3. Numerical Results

In this section, we present illustrative examples which compares the estimation performance of PTA scheme as compared to ETA scheme. In Fig 5.4, optimal time allocations for the PTA scheme are both obtained by maximizing the upperbound on Mutual Information and with respect to individual Mutual Information. When PTA scheme is executed by maximizing the upperbound on Mutual Information, the entire transmission is partitioned among few informative sensors. If the observation of such sensors are lower than their decision thresholds, these sensors don't transmit and time allocated for their transmission is wasted. As seen in Table 5.3, all time is allocated most informative sensor by maximizing the upperbound on Mutual Information. Thus, only one sensor has high correctly transmission probability $P_{1|1}$.

As a consequence, PTA maximizing the upperbound on Mutual Information yields the worst estimation performance. Not shown here, a similar result is also obtained when we directly maximize the exact mutual information. An alternative approach is to determine the time allocation of each sensor with respect to its individual Mutual Information. By doing so, time allocation of each sensor becomes fairer than as obtained by maximizing the upperbound on Mutual Information as shown in Table 5.3. Simulation results show that, for $N = 9$ sensors in the WSN, using PTA with respect to individual Mutual Information, provides better estimation performance as compared to ETA where the sensor decision thresholds are obtained by maximizing the mutual information or upperbound on mutual information. We obtain a similar result in Fig 5.5 where for $N = 16$ sensors, estimation performance of PTA is better than that of ETA. Note that when the number of sensors in the WSN is relatively large, the allocated time duration per each sensor become very short. Therefore, when the

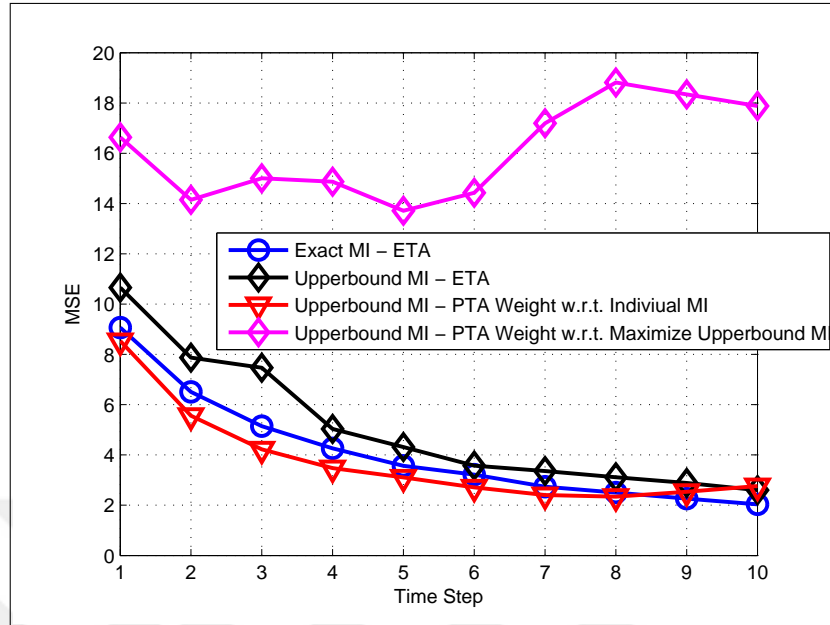


Figure 5.4. Performance Comparison between ETA and PTA, $N = 9$.

Table 5.3. Probabilities of the received binary decisions and PTA values of each nodes at one step of tracking

Sensor Nodes	Sensor Threshold	Weight w.r.t. maximize MI		Weight w.r.t. Individual MI	
		PTA	$P_{1 1}$	PTA	$P_{1 1}$
Node 1	70.71	1.00	0.96	0.65	0.93
Node 2	11.04	0.00	0.01	0.12	0.71
Node 3	4.54	0.00	0.01	0.01	0.11
Node 4	9.95	0.00	0.01	0.12	0.70
Node 5	8.31	0.00	0.01	0.07	0.54
Node 6	4.16	0.00	0.01	0.01	0.09
Node 7	4.54	0.00	0.01	0.01	0.11
Node 8	4.16	0.00	0.01	0.01	0.09
Node 9	3.33	0.00	0.01	0.00	0.03

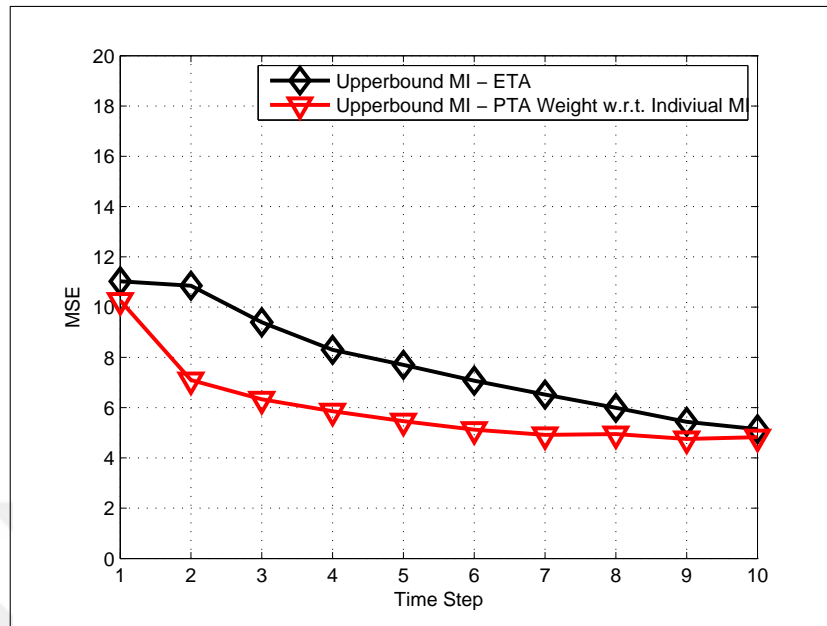


Figure 5.5. Performance Comparison between ETA and PTA, $N = 16$.

number of sensors in the network is large, we need to first select a number of informative sensors and turn-off the sensors which are far from the target of interest. In Fig. 5.6, we first select N_A sensors among N sensors in the WSN where N_A represents the number of time allocated sensors. Our simulation results show that when N_A is small, the selected sensors receive enough time to transmit their binary decisions successfully on the other hand if their measurements are less than the threshold, fusion center may get insufficient decisions from sensors. As N_A further increases, PTA provides better estimation performance than that of ETA. For large values of N_A close to N estimation error increases as a result of small transmission duration per each sensor, hence increasing the probability of transmission errors.

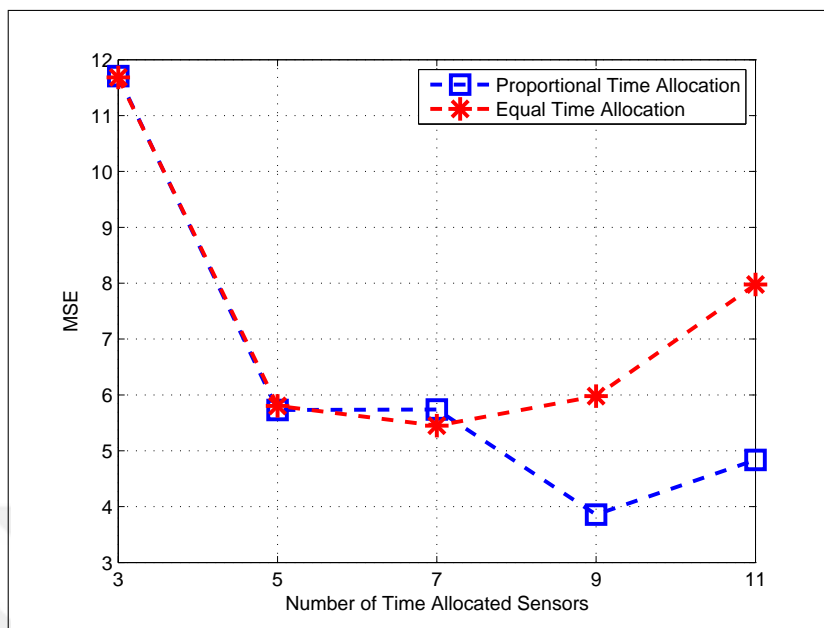


Figure 5.6. Performance of ETA and PTA with sensor selection

6. CONCLUSION AND FUTURE RESEARCH DIRECTIONS

In this thesis, efficient resource managements with adaptive binary quantizer design problem under single-hop and 2-hop links for target tracking in WSNs have been investigated. The main aim of the thesis is to provide significant savings in the limited resources of network while keeping good estimation performance for target tracking.

We first solved adaptive binary quantizer design problem under single-hop links for target tracking using multiobjective optimization methods. A good trade off solution between estimation error and sum of sensor transmission probabilities were obtained by the help of NBI method which takes less time than NSGA-II. Simulation results show that number of transmitting sensors are reduced significantly as well as ensuring a good estimation performance.

Energy consumption performance has been also investigated while considering energy depletion in hardware of sensor nodes under single-hop and 2-hop links to prolong life time of network. While energy burden on sensor nodes were significantly reduced under cluster based 2-hop transmission, transmitting under single-hop caused more energy consumption on sensors especially which are far away from the FC. While 2-hop significantly reduce energy consumption of sensor nodes except CHs in cluster, overall energy consumption of network becomes higher than single-hop. This because because less energy consumption occurs when some sensors send directly to FC instead of transmission over CHs. Thus, we prefer MTEP where sensors' data follow less required energy path to prevent fast depletion of the sensors which are far away from FC. The considered MTEP is a composition of single-hop and 2-hop transmission, so sensor's data follow either single-hop or 2-hop link to reach FC based on required energy. Thus, MTEP curtailed excessive energy consumption on cluster heads under 2-hops by routing some sensors' information to use single-hop transmission. Furthermore, by using MOP we forced less informative sensors to stay silent. Thus, we reduce energy consumption by impeding less informative sensors about target location from unnecessary transmission to CHs and FC. We observed that even though circuit energy is considered, MTEP are more energy efficient than single-hop transmission in terms of overall energy

consumption of network.

Adaptive binary quantizer design problem was also solved while considering wireless channel effects. In addition, we obtained sensor decision thresholds by different information metrics with comparing estimation performances and computation times. As we observed that optimal metrics of MI and FI are computationally heavy, we also used suboptimal metrics version of them. By using these suboptimal metrics, the objective function becomes decoupled among sensors and sensor decision thresholds were obtained easily. For the case where the total transmission duration is equally distributed among sensors in a TDMA manner, our simulation results showed that maximizing the mutual information or minimizing the trace of C-PCRLB yield similar estimation performance, where among the less complex metrics the upperbound on mutual information yields better estimation performance than the lower bound on the trace of C-PCRLB. Based information metrics, we proposed a proportional time allocation strategy where the time allocated to each sensor is determined as a function of its information. So that the informative sensors acquires more time to decrease their transmission errors and the non-informative sensors are forced to stay silent. In our simulation results show that, when the number of sensors in the WSN is relatively large, proportional time allocation improves the estimation performance as compared to equal time allocation. However, for further increasing in number of selected sensors both allocation performance got worse on estimation performance due to small transmission duration per each sensor that result in increased probability of transmission errors.

As a future work, we want to deal with larger sensor networks in which massive traffic burden occurs in cluster head nodes while considering energy consumption in hardware. We will propose an energy based adaptive transmission by considering only informative sensors about target location. Cluster heads would make a decision about the sensors' data. If the information is distorted under wireless channel impairments, cluster heads would not transmit such data to destination node. Thus, apart from improvements on estimation performance, energy consumption in CHs can also be reduced by cancelling transmission of distorted signal to FC. On the other hand, knowing that sensors' measurements have to reach destination node at a certain time for target tracking, achieving low transmission latency is also a big challenge need to be alleviated for moving targets.

REFERENCES

1. K. Sohraby, D. Minoli, and T. Znati. *Wireless Sensor Networks: Technology, Protocols, and Applications*, John Wiley and Sons, Inc., Hoboken, New Jersey, 2007.
2. S. Joshi and S. Boyd. Sensor Selection via Convex Optimization. *IEEE Transactions on Signal Processing*, 2:451-462, February 2009.
3. E. Masazade, R. Niu, and P. K. Varshney. Dynamic Bit Allocation for Object Tracking in Wireless Sensor Networks. *IEEE Transactions on Signal Processing*, 10:5048-5063, 2012.
4. R. Jiang and B. Chen. Fusion of Censored Decisions in Wireless Sensor Networks. *IEEE Transactions on Wireless Communications*, 6:2668-2673, November 2005.
5. I. Demirkol, C. Ersoy, and F. Alagoz. Mac Protocols for Wireless Sensor Networks: A Survey. *IEEE Communications Magazine*, 4:115-121, April 2006.
6. P. Huang, L. Xiao, S. Soltani, M.W. Mutka, and N. Xi. The Evolution of Mac Protocols in Wireless Sensor Networks: A Survey. *IEEE Communications Surveys Tutorials*, 1:101-120, 2013.
7. L. Song and D. Hatzinakos. A Cross-Layer Architecture of Wireless Sensor Networks for Target Tracking. *IEEE/ACM Transactions on Networking*, 1:145-158, February 2007.
8. P. Cheng, F. Zhang, J. Chen, Y. Sun, and X. Shen. A Distributed Tdma Scheduling Algorithm for Target Tracking in Ultrasonic Sensor Networks. *IEEE Transactions on Industrial Electronics*, 9:3836-3845, September 2013.
9. L. Orihuela, F. Gmez-Estern, and F. R. Rubio. Scheduled Communication in Sensor Networks. *IEEE Transactions on Control Systems Technology*, 2:801-808, March 2014.
10. Y. Zheng, N. Cao, T. Wimalajeewa, and P. K. Varshney. Compressive Sensing Based Probabilistic Sensor Management for Target Tracking in Wireless Sensor Networks. *IEEE*

Transactions on Signal Processing, 22:6049-6060, November 2015.

11. R. Niu and P. K. Varshney. Target Location Estimation in Sensor Networks with Quantized Data. *IEEE Transactions on Signal Processing*, 12:4519-4528, December 2006.
12. O. Ozdemir, R. Niu, and P. K. Varshney. Adaptive Local Quantizer Design for Tracking in a Wireless Sensor Network. *2008 IEEE 42nd Asilomar Conference on Signals, Systems and Computers*, 1202-1206, October 2008,
13. M. Vemula, M. Bugallo, and P. Djuric. Particle Filtering-Based Target Tracking in Binary Sensor Networks Using Adaptive Thresholds. *2007 IEEE 2nd International Workshop on Computational Advances in Multi-Sensor Adaptive Processing*, 17-20, December 2007.
14. S. Liu, E. Masazade, X. Shen, and P. K. Varshney. Adaptive Non-Myopic Quantizer Design for Target Tracking in Wireless Sensor Networks. *2013 IEEE Asilomar Conference on Signals, Systems and Computers*, 1085-1089, November 2013.
15. K. Mukherjee, A. Ray, T. Wettergren, S. Gupta, and S. Phoha. Real-Time Adaptation of Decision Thresholds in Sensor Networks for Detection of Moving Targets. *Automatica*, 1:185-191, 2011.
16. C. Kreucher, A. Hero, K. Kastella, and M. Morelande. An Information-Based Approach to Sensor Management in Large Dynamic Networks. *Proceedings of the IEEE*, 5:978-999, May 2007.
17. G. M. Hoffmann and C. J. Tomlin. Mobile Sensor Network Control Using Mutual Information Methods and Particle Filters. *IEEE Transactions on Automatic Control*, 1:32-47, January 2010.
18. J. Williams, J. Fisher, and A. Willsky. Approximate Dynamic Programming for Communication-Constrained Sensor Network Management. *IEEE Transactions on Signal Processing*, 8:4300-4311, August 2007.

19. Y. Zhang and Q. Ji. Efficient Sensor Selection for Active Information Fusion. *IEEE Transactions on Systems, Man, and Cybernetics, Part B: Cybernetics*, 3:719-728, June 2010.
20. M. Hernandez, T. Kirubarajan, and Y. Bar-Shalom. Multisensor Resource Deployment Using Posterior CramEr-Rao Bounds. *IEEE Transactions on Aerospace and Electronic Systems*, 2:399-416, April 2004.
21. L. Zuo, R. Niu, and P. K. Varshney. Posterior Crlb Based Sensor Selection For Target Tracking in Sensor Networks. *2007 IEEE International Conference on Acoustics, Speech and Signal Processing, ICASSP*, II-1041-II-1044, 2007.
22. L. Zuo, R. Niu, and P. K. Varshney. A Sensor Selection Approach for Target Tracking in Sensor Networks with Quantized Measurements. in Proc. *2007 IEEE International Conference on Acoustics, Speech and Signal Processing, ICASSP*, 2521-2524, April 2008.
23. A. Kose and E. Masazade. Adaptive Sampling with Sensor Selection for Target Tracking in Wireless Sensor Networks. *2014 IEEE 48th Asilomar Conference on Signals, Systems and Computers*, 909-913, November 2014.
24. E. Masazade, R. Niu, P. K. Varshney, and M. Keskinöz. Energy Aware Iterative Source Localization for Wireless Sensor Networks. *IEEE Transactions on Signal Processing*, 9:4824-4835, September 2010.
25. W. Heinzelman, A. Chandrakasan, and H. Balakrishnan. Energy Efficient Communication Protocol for Wireless Microsensor Networks. *Proceedings of the 33rd Annual Hawaii International Conference on System Sciences*, 8020-830, January 2000.
26. S. Aeron, V. Saligrama, and D. A. Castanon. Energy Efficient Policies for Distributed Target Tracking in Multihop Sensor Networks. *IEEE 45th Conference on Decision and Control*, 380-385, December 2006.
27. M. Mahir and H. Daryoush. Transmission Power Control in Multihop Wireless Sensor Networks. *2011 Third International Conference on Ubiquitous and Future Networks (ICUFN)*,

25-30, June 2011.

28. X. Yang, R. Niu, E. Masazade, and P. K. Varshney. Channel-Aware Tracking in Multihop Wireless Sensor Networks with Quantized Measurements. *IEEE Transactions on Aerospace and Electronic Systems*, 4:2353-2368, October 2013.

29. R. Min and A. P. Chandrakasan. Top Five Myths About The Energy Consumption of Wireless Communication. *ACM Mobile Computing and Communications Review*, pages 65-67, 2002.

30. B. Chen, L. Tong, and P. Varshney. Channel-Aware Distributed Detection in Wireless Sensor Networks. *IEEE Signal Processing Magazine*, 4:16-26, July 2006.

31. B. Liu and B. Chen. Channel-Optimized Quantizers for Decentralized Detection in Sensor Networks. *IEEE Transactions on Information Theory*, 7:3349-3358, July 2006.

32. R. Niu, B. Chen, and P. Varshney. Fusion of Decisions Transmitted over Rayleigh Fading Channels in Wireless Sensor Networks. *IEEE Transactions on Signal Processing*, 3:1018-1027, March 2006.

33. O. Ozdemir, R. Niu, and P. K. Varshney. Channel Aware Target Localization with Quantized Data in Wireless Sensor Networks. *IEEE Transactions on Signal Processing*, 3:1190-1202, March 2009.

34. O. Ozdemir, R. Niu, and P. K. Varshney. Tracking in Wireless Sensor Networks Using Particle Filtering: Physical Layer Considerations. *IEEE Transactions on Signal Processing*, 5:1987-1999, May 2009.

35. R. Madan, S. Cui, S. Lall, and N. A. Goldsmith. Cross-Layer Design for Lifetime Maximization in Interference-Limited Wireless Sensor Networks. *IEEE Transactions on Wireless Communications*, 11:3142-3152, November 2006.

36. X. Jianming, W. Liu, H. Yun, and Q. Gaorong. Energy-Efficient Sensor Scheduling

Scheme for Target Tracking in Wireless Sensor Networks. *The 26th Chinese Control and Decision Conference*, 1869-1874, May 2014.

37. B. Zakiruli, W. Guojun, and V. Athanasios. Local Area Prediction-Based Mobile Target Tracking in Wireless Sensor Networks. *IEEE Transactions on Computers*, 7:1968-1982, July 2014.

38. R. Niu and P. K. Varshney. Distributed Detection and Fusion in A Large Wireless Sensor Network of Random Size. *EURASIP Journal on Wireless Communications and Networking*, 4:462-472, 2005.

39. Y. Zheng, O. Ozdemir, R. Niu, and P. K. Varshney. New Conditional Posterior Cramerrao Lower Bounds for Nonlinear Sequential Bayesian Estimation. *IEEE Transactions on Signal Processing*, 10:5549-5556, October 2012.

40. E. Masazade, R. Rajagopalan, P. K. Varshney, C. Mohan, G. Sendur, and M. Keskinoz. A Multiobjective Optimization Approach to Obtain Decision Thresholds for Distributed Detection in Wireless Sensor Networks. *IEEE Transactions on Systems, Man, and Cybernetics, Part B: Cybernetics*, 2:44-457, April 2010.

41. I. Das and J. Dennis. Normal-Boundary Interaction: A New Method for Generating The Pareto Surface in Nonlinear Multicriteria Optimization Problems. *SIAM Journal of Optimization*, 631-657, 1998.

42. E. Rigoni and S. Poles. NBI and MOGA-II, Two Complementary Algorithms for Multi-Objective Optimizations. In: J. Branke, K. Deb, K. Miettinen, and R. E. Steuer, Eds, editors, *Practical Approaches to Multi-Objective Optimization, ser*, Dagstuhl Seminar Proceedings 04461, Internationales Begegnungs- und Forschungszentrum für Informatik (IBFI), Schloss Dagstuhl, Germany, 2005

43. K. Deb, A. Pratap, S. Agarwal, and T. Meyarivan. A Fast and Elitist Multiobjective Genetic Algorithm: NSGA-II. *IEEE Transactions on Evolutionary Computation*, 2:182-197, April 2002.

44. M. Arulampalam, S. Maskell, N. Gordon, and T. Clapp. A Tutorial on Particle Filters for Online Nonlinear/Non-Gaussian Bayesian Tracking. *IEEE Transactions on Signal Processing*, 2:174-188, February 2002.
45. Y. Bar-Shalom, P. K. Willett, and X. Tian. *Tracking and Data Fusion: A Handbook of Algorithms*. YBS Publishing, Storrs, CT, 2011.
46. J. Fang and H. Li. Power Constrained Distributed Estimation with Correlated Sensor Data. *IEEE Transactions on Signal Processing*, 8:3292-3297, August 2009.
47. X. Shen and P. K. Varshney. Sensor Selection Based on Generalized Information Gain for Target Tracking in Large Sensor Networks. *IEEE Transactions on Signal Processing*, 2:363-375, January 2014.
48. N. Cao, E. Masazade, and P. K. Varshney. A Multiobjective Optimization Based Sensor Selection Method for Target Tracking in Wireless Sensor Networks. *16th International Conference on Information Fusion (FUSION)*, 974-980, July 2013.
49. P. Tan, M. Steinbach, and V. Kumar. *Introduction to Data Mining*, Pearson, 2005.
50. S. M. Kay. *Fundamentals of Statistical Signal Processing, vol. II: Detection Theory*, Prentice Hall, New Jersey 1998.
51. T. M. Cover and J. A. Thomas. *Elements Of Information Theory*, John Wiley and Sons, Inc., Hoboken, New Jersey, 2006.

APPENDIX A: MI UNDER NON-IDEAL CHANNELS

If the wireless channel is not ideal the mutual information in Eqn. 2.12 can be expressed as,

$$I(\mathbf{x}_{t+1}, \mathbf{R}_{t+1}) = H(\mathbf{R}_{t+1}) - H(\mathbf{R}_{t+1}|\mathbf{x}_{t+1}) \quad (\text{A.1})$$

where $H(\mathbf{R}_{t+1})$ is the entropy of \mathbf{R}_{t+1} and $H(\mathbf{R}_{t+1}|\mathbf{x}_{t+1})$ is the conditional entropy of \mathbf{R}_{t+1} given the target location \mathbf{x}_{t+1} . Firstly, $H(\mathbf{R}_{t+1})$ is computed from,

$$\begin{aligned} H(\mathbf{R}_{t+1}) &= - \sum_{\mathbf{R}_{t+1}} P(\mathbf{R}_{t+1}) \log_2 P(\mathbf{R}_{t+1}) \\ &= - \sum_{r_1=0}^1 \dots \sum_{r_N=0}^1 P(R_{1,t+1} = r_1, \dots, R_{N,t+1} = r_N) \\ &\quad \times \log_2 P(D_{1,t+1} = r_1, \dots, R_{N,t+1} = r_N) \end{aligned} \quad (\text{A.2})$$

where

$$\begin{aligned} &P(R_{1,t+1} = r_1, \dots, R_{N,t+1} = r_N) \\ &= \int P(R_{1,t+1} = r_1, \dots, R_{N,t+1} = r_N | \mathbf{x}_{t+1}) p(\mathbf{x}_{t+1}) d\mathbf{x}_{t+1} \\ &= \int \left(\prod_{i=1}^N P(R_{i,t+1} = r_i | \mathbf{x}_{t+1}) \right) p(\mathbf{x}_{t+1}) d\mathbf{x}_{t+1} \end{aligned} \quad (\text{A.3})$$

Using the particle filter approximation of $p(\mathbf{x}_{t+1}) \approx p(\mathbf{x}_{t+1}|\mathbf{R}_t)$, $P(R_{1,t+1} = r_1, \dots, R_{N,t+1} = r_N)$ is approximated by

$$P(R_{1,t+1} = r_1, \dots, R_{N,t+1} = r_N) \approx \sum_{s=1}^{N_s} w_{t+1}^s \times \left[\prod_{i=1}^N \left(\sum_{d_i=0}^1 P(R_{i,t+1} = r_i | D_{i,t+1} = d_i) P(D_{i,t+1} = d_i | \mathbf{x}_{t+1}^s) \right) \right] \quad (\text{A.4})$$

Secondly, the conditional entropy $H(\mathbf{R}_{t+1}|\mathbf{x}_{t+1})$ is computed as,

$$\begin{aligned} H(\mathbf{R}_{t+1}|\mathbf{x}_{t+1}) &= - \int_{\mathbf{x}_{t+1}} \sum_{\mathbf{R}_{t+1}} p(\mathbf{R}_{t+1}, \mathbf{x}_{t+1}) \log_2 p(\mathbf{R}_{t+1}|\mathbf{x}_{t+1}) d\mathbf{x}_{t+1} \\ &= - \int_{\mathbf{x}_{t+1}} \sum_{\mathbf{R}_{t+1}} [p(\mathbf{R}_{t+1}|\mathbf{x}_{t+1}) \log_2 p(\mathbf{R}_{t+1}|\mathbf{x}_{t+1})] p(\mathbf{x}_{t+1}) d\mathbf{x}_{t+1} \\ &= - \int_{\mathbf{x}_{t+1}} \sum_{r_1=0}^1 \dots \sum_{r_N=0}^1 \left[\left(\prod_{i=1}^N P(R_{i,t+1} = r_i | \mathbf{x}_{t+1}) \right) \right. \\ &\quad \left. \log_2 \left(\prod_{i=1}^N P(R_{i,t+1} = r_i | \mathbf{x}_{t+1}) \right) \right] p(\mathbf{x}_{t+1}) d\mathbf{x}_{t+1} \\ &= - \int_{\mathbf{x}_{t+1}} \sum_{i=1}^N \sum_{r_i=0}^1 [P(R_{i,t+1} = r_i | \mathbf{x}_{t+1}) \log_2 P(R_{i,t+1} = r_i | \mathbf{x}_{t+1})] \\ &\quad \times p(\mathbf{x}_{t+1}) d\mathbf{x}_{t+1} \\ &= - \int_{\mathbf{x}_{t+1}} \sum_{i=1}^N \sum_{r_i=0}^1 \left[\left(\sum_{d_i=0}^1 P(R_{i,t+1} = r_i | D_{i,t+1} = d_i) P(D_{i,t+1} = d_i | \mathbf{x}_{t+1}) \right) \right. \\ &\quad \left. \log_2 \left(\sum_{d_i=0}^1 P(R_{i,t+1} = r_i | D_{i,t+1} = d_i) P(D_{i,t+1} = d_i | \mathbf{x}_{t+1}) \right) \right] p(\mathbf{x}_{t+1}) d\mathbf{x}_{t+1} \quad (\text{A.5}) \end{aligned}$$

APPENDIX B: FI UNDER NON-IDEAL CHANNELS

\mathbf{J}_{t+1} has the form,

$$E \{ [\hat{\mathbf{x}}_{t+1} - \mathbf{x}_{t+1}] [\hat{\mathbf{x}}_{t+1} - \mathbf{x}_{t+1}]^T \} \geq \mathbf{J}_{t+1}^{-1} \quad (\text{B.1})$$

where \mathbf{J}_{t+1} is the 4×4 Fisher information matrix (FIM). If the channel is not ideal, \mathbf{J}_{t+1} in Eqn. 2.18 is defined by,

$$\begin{aligned} \mathbf{J}_{t+1} &\triangleq E_{p(\mathbf{x}_{t+1}, \mathbf{R}_{t+1})} \left[-\nabla_{\mathbf{x}_{t+1}}^{\mathbf{x}_{t+1}} \log p(\mathbf{x}_{t+1}, \mathbf{R}_{t+1}) \right] \\ &= - \underbrace{\int_{\mathbf{x}_{t+1}} \sum_{\mathbf{R}_{t+1}} P(\mathbf{R}_{t+1} | \mathbf{x}_{t+1}) \left[-\nabla_{\mathbf{x}_{t+1}}^{\mathbf{x}_{t+1}} \log P(\mathbf{R}_{t+1} | \mathbf{x}_{t+1}) \right] p(\mathbf{x}_{t+1}) d\mathbf{x}_{t+1}}_{\triangleq \mathbf{J}_{t+1}^D} \\ &\quad - \underbrace{\int_{\mathbf{x}_{t+1}} \left[-\nabla_{\mathbf{x}_{t+1}}^{\mathbf{x}_{t+1}} \log p(\mathbf{x}_{t+1}) \right] p(\mathbf{x}_{t+1}) d\mathbf{x}_{t+1}}_{\triangleq \mathbf{J}_{t+1}^P} \end{aligned} \quad (\text{B.2})$$

where \mathbf{J}_{t+1} can be decomposed into data part, \mathbf{J}_{t+1}^D and prior part, \mathbf{J}_{t+1}^P . Data part of the Fisher Information can be further written as,

$$\begin{aligned} \mathbf{J}_{t+1}^D &= - \int_{\mathbf{x}_{t+1}} \sum_{r_1=0}^1 \cdots \sum_{r_N=0}^1 \left(\prod_{i=1}^N P(R_{i,t+1} = r_i | \mathbf{x}_{t+1}) \right) \\ &\quad \left[-\nabla_{\mathbf{x}_{t+1}}^{\mathbf{x}_{t+1}} \log \left(\prod_{i=1}^N P(R_{i,t+1} = r_i | \mathbf{x}_{t+1}) \right) \right] p(\mathbf{x}_{t+1}) d\mathbf{x}_{t+1} \\ &= \sum_{i=1}^N \left\{ - \int_{\mathbf{x}_{t+1}} \sum_{r_i=0}^1 P(R_{i,t+1} = r_i | \mathbf{x}_{t+1}) \left[-\nabla_{\mathbf{x}_{t+1}}^{\mathbf{x}_{t+1}} \log P(R_{i,t+1} = r_i | \mathbf{x}_{t+1}) \right] \right. \\ &\quad \left. \times p(\mathbf{x}_{t+1}) d\mathbf{x}_{t+1} \right\} \end{aligned} \quad (\text{B.3})$$

where \mathbf{J}_{t+1}^D is equal to sum of each sensors contribution to the Fisher Information, $\mathbf{J}_{i,t+1}^D$. Using the properties given in [11], $\mathbf{J}_{i,t+1}^D$ can be written as,

$$\begin{aligned}
\mathbf{J}_{i,t+1}^D &= \\
&\int_{\mathbf{x}_{t+1}} \sum_{r_i=0}^1 \frac{1}{P(R_{i,t+1} = r_i | \mathbf{x}_{t+1})} \left(\frac{\partial}{\partial \mathbf{x}_{t+1}} P(R_{i,t+1} = r_i | \mathbf{x}_{t+1}) \right)^2 p(\mathbf{x}_{t+1}) d\mathbf{x}_{t+1} \\
&= \int_{\mathbf{x}_{t+1}} \sum_{r_i=0}^1 \frac{1}{\left(\sum_{d_i=0}^1 P(R_{i,t+1} = r_i | D_{i,t+1} = d_i) P(D_{i,t+1} = d_i | \mathbf{x}_{t+1}) \right)} \\
&\quad \left[\sum_{d_i=0}^1 P(R_{i,t+1} = r_i | D_{i,t+1} = d_i) \left(\frac{\partial}{\partial \mathbf{x}_{t+1}} P(D_{i,t+1} = d_i | \mathbf{x}_{t+1}) \right) \right]^2 \\
&\quad \times p(\mathbf{x}_{t+1}) d\mathbf{x}_{t+1} \tag{B.4}
\end{aligned}$$

where detailed derivation of $\frac{\partial}{\partial \mathbf{x}_{t+1}} P(D_{i,t+1} = d_i | \mathbf{x}_{t+1})$ is given in [3]. Using the particle filter approximation $\mathbf{J}_{i,t+1}^D$ is approximated by

$$\begin{aligned}
\mathbf{J}_{i,t+1}^D &\approx \\
&\sum_{s=1}^{N_S} \frac{1}{N_S} \left\{ \sum_{r_i=0}^1 \frac{1}{\left(\sum_{d_i=0}^1 P(R_{i,t+1} = r_i | D_{i,t+1} = d_i) P(D_{i,t+1} = d_i | \mathbf{x}_{t+1}^s) \right)} \right. \\
&\quad \left. \left[\sum_{d_i=0}^1 P(R_{i,t+1} = r_i | D_{i,t+1} = d_i) \left(\frac{\partial}{\partial \mathbf{x}_{t+1}} P(D_{i,t+1} = d_i | \mathbf{x}_{t+1}^s) \right) \right]^2 \right\} \tag{B.5}
\end{aligned}$$

In summary, \mathbf{J}_{t+1} is written as,

$$\begin{aligned}
\mathbf{J}_{t+1} &= \mathbf{J}_{t+1}^D + \mathbf{J}_{t+1}^P \\
&= \sum_{i=1}^N \mathbf{J}_{i,t+1}^D + \mathbf{J}_{t+1}^P \tag{B.6}
\end{aligned}$$